Winter 2022

Characterization of phenotypic traits related to loss-of-function and ectopic expression of bHLH093 and bHLH061 in Arabidopsis thaliana

Leila Belhadjali
Western Washington University, nwhiker@live.com

Recommended Citation

Characterization of phenotypic traits related to loss-of-function and ectopic expression of bHLH093 and bHLH061 in *Arabidopsis thaliana*

By
Leila Belhadjali

Accepted in Partial Completion
of the Requirements for the Degree
Master of Science

ADVISORY COMMITTEE

Dr. Lynn Pillitteri, Chair

Dr. Sandra Schulze

Dr. Anu Singh-Cundy

GRADUATE SCHOOL

David L. Patrick, Dean

Master's Thesis

In presenting this thesis in partial fulfillment of the requirements for a master's degree at Western Washington University, I grant to Western Washington University the non-exclusive royalty-free right to archive, reproduce, distribute, and display the thesis in any and all forms, including electronic format, via any digital library mechanisms maintained by WWU.

I represent and warrant this is my original work, and does not infringe or violate any rights of others. I warrant that I have obtained written permissions from the owner of any third party copyrighted material included in these files.

I acknowledge that I retain ownership rights to the copyright of this work, including but not limited to the right to use all or part of this work in future works, such as articles or books.

Library users are granted permission for individual, research and non-commercial reproduction of this work for educational purposes only. Any further digital posting of this document requires specific permission from the author.

Any copying or publication of this thesis for commercial purposes, or for financial gain, is not allowed without my written permission.

Leila Belhadjali
28 February 2022

Characterization of phenotypic traits related to loss-of-function and ectopic expression of bHLH093 and bHLH061 in *Arabidopsis thaliana*

A Thesis
Presented to
The Faculty of
Western Washington University

In Partial Fulfillment
Of the Requirements for the Degree
Master of Science

by
Leila Belhadjali
28 February 2022

Abstract

bHLH093 and *bHLH061* are members of sub-group IIIb of basic helix-loop-helix (bHLH)

Arabidopsis thaliana transcription factors. Although bHLH proteins are the second largest

transcription factor family in Arabidopsis, only a small proportion of them have been

functionally characterized. Here, we investigated the phenotypic impact of bHLH061 and

bHLH093 ectopic overexpression and loss-of-function to confirm previously published

results and provide new insight into their role in development. bHLH093 and bHLH061

are homologs of two stomatal development genes, SCREAM1/ICE1 and SCREAM2 and have

been shown to dimerize with two master regulators of stomata development, FAMA and

MUTE. While no evidence was found in this study to implicate the involvement of bHLH061

and bHLH03 stomatal development, we determined that overexpression of these bHLH

genes has a significant impact on flowering time, apical dominance, and root growth under

long-day conditions. Taken together, our data generally confirmed the published analysis of

bHLH093 and bHLH061 function in gibberellin- mediated promotion of flowering and

reproductive transition, but also provided a potentially new avenue of future investigation

looking at the impact of these genes on root development.

Acknowledgements

I would like to express my deepest appreciation to my thesis advisor, Dr. Lynn Pillitteri for her advice, patience, encouragement, and support. Her help and instruction in the lab were invaluable. Her editing skills improved this manuscript considerably.

I also want to thank my committee members Dr. Sandra Schulze and Dr. Anu Singh-Cundy for their suggestions, feedback, and advice.

I want to acknowledge (then) undergraduate research assistants Jordan Wagner, Jesika Smith, and Olivia Thompson for all their assistance in the lab.

My research was supported by a grant from the Fraser Fund, for which I am grateful.

David, Anne-Chloe, Perry, and Linnea: I couldn't have done it without your love and patience.

Table of contents

List of Tables

List of Figures

Introduction

Plant morphogenesis

An organism's final form is the result of interplay between intrinsic developmental programs and external environmental influences. Morphogenesis (the generation of form) is a process that controls the spatial distribution of cells by regulating cell division, cell growth, and differentiation. The ultimate outcome of this process is the acquisition of multiple tissues and organs with distinct functions. Investigation of genes that regulate morphogenesis is fundamental to the field of developmental biology.

Although both plant and animals undergo extensive development during embryogenesis to establish their body plans, plants have the extraordinary capacity to generate organs and tissues throughout their entire lives (Dinneny and Benfey, 2008). This capacity arises from structures called meristems consisting of indeterminant, undifferentiated cells that generate the majority of biomass and organs of the mature plant. Meristematic cells can be considered analogous to stem cells in animals: they are pluripotent and give rise to the different cell types (Groß-Hardt and Laux, 2003; Mayer et al., 1998). Plants have two primary meristems located at the apical shoot and root tip, which give rise to the primary vertical axis of the plant body. In addition, numerous lateral or secondary meristematic regions contribute to plant body architecture and are important for plants to sense environmental conditions and adapt developmental programs accordingly (Scofield and Murray, 2006).

Large data set analysis and -omics advances have revolutionized our insight into gene expression and cooperating gene networks. However, a vast number of annotated genes in plants have not been assigned a specific functional role. Functional characterization of genes that regulate morphogenesis is an important field of study necessary to broaden our understanding of how plants adapt patterning programs to changing conditions (Cheng and Perocchi, 2015; Dey et al., 2015; Dinneny and Benfey, 2008; Wood et al.).

Arabidopsis thaliana as model system for development

Arabidopsis thaliana is a plant of the mustard family (*Brassicaceae*) that is the most widely used model organism in plants. Arabidopsis is extensively used to investigate questions related to plant science, genetics, development, and evolution. Importantly, much of the knowledge gained from the research in Arabidopsis has helped further our understanding of similar processes in other systems and commercially important crops (Cantín et al., 2007; Lee et al., 2014; Mitre et al., 2021). For example, the Arabidopsis MYB12 (AtMYB12) transcription factor activates the production of flavanols, which are known to improve cardiovascular health in mammals. Expressing AtMYB12 in tomato plants produced a commercially edible crop with increased flavanol content (Luo et al., 2008; Perez-Vizcaino and Duarte, 2010). Beyond plants, Arabidopsis has also helped advance work involving the biochemical and molecular processes of human diseases (Belfield et al., 2018). Although advances in sequencing technology and DNA-based editing tools allow other plants to be analyzed in a way that was once only feasible in Arabidopsis

(Jiang et al., 2013), currently the extensive body of work produced over the last 30 years maintains Arabidopsis as a critical research tool for plants. (Jiang et al., 2013; Luo et al., 2008; Perez-Vizcaino and Duarte, 2010).

Some of the benefits of Arabidopsis are its small size (15cm-20cm height) and relatively short life cycle (~eight weeks from seed to seed). It can be easily grown under artificial lights, is genetically transformed in a simple manner, and has a small genome (114 Mbp) that is very well characterized (Clough and Bent, 1998; Meinke et al., 1998; The *Arabidopsis* Genome Initiative, 2000). In addition, Arabidopsis is self-fertile and can produce thousands of seeds (Van Daele et al., 2012). These reasons make Arabidopsis an excellent system to study the role of individual genes on morphogenesis which can then be applied to broader questions in the plant community (Chater et al., 2017; Lau and Bergmann, 2012; Pillitteri et al., 2007; Ran et al., 2013).

Genetic Regulation of Development; bHLH proteins

In all organisms, transcription factors play a critical role in the activation of gene networks necessary to carry out developmental programs. Transcription factors make up about 7.4% of the Arabidopsis genome (Mitsuda and Ohme-Takagi, 2009) and determining how these factors define and coordinate different developmental events is an active area of research. Basic helix-loop-helix (bHLH) proteins are one of the largest family of transcription factors and are ubiquitously found in organisms from yeast to humans. This family of transcription factors are known players in a wide number of processes including neurogenesis, myogenesis, cell proliferation, cell differentiation, and cell lineage determination. Specifically, these proteins often function as intrinsic regulators of cellular

"decision" making (Atchley and Fitch, 1997; Jones, 2004; Kanaoka et al., 2008; Ledent et al., 2002; Massari and Murre, 2000, 2000; Toledo-Ortiz et al., 2003).

The bHLH motif was first identified in mice (Murre et al., 1989) and is the general motif that defines this large group of dimerizing transcription factors. Additional categorization has been done using evolutionary relationships, DNA binding specificity and the presence of additional protein domains (Heim et al., 2003; Toledo-Ortiz et al., 2003). The bHLH domain is made up of approximately 60 amino acids consisting of a basic region followed by a helix-loop-helix region (Atchley and Fitch, 1997; Hao et al., 2021; Murre et al., 1989). The basic region contains approximately 15 mostly basic residues located at the N-terminal of the domain and is an absolute requirement for DNA binding. Two highly conserved amino acids in the basic region, a glutamate and an arginine residue, mediate DNA binding specificity (Murre, 2019) to the bHLH E-box consensus sequence, CANNTG (Atchley and Fitch, 1997; Toledo-Ortiz et al., 2003). But the binding specificity of individual bHLH proteins depends on the nature of the two non-specific nucleotides of the consensus sequence and additional nucleotides in the vicinity of the E-box (Gordân et al., 2013; Toledo-Ortiz et al., 2003). The HLH region is located C-terminal to the basic domain and functions in protein homo- and hetero- dimerization. (Atchley and Fitch, 1997; Splettstoesser, 2007; Toledo-Ortiz et al., 2003). The ability to bind with multiple partners allows for the potential to function in multiple pathways.

bHLH proteins in Arabidopsis

Basic helix-loop-helix proteins represent the second largest transcription factor family in Arabidopsis, consisting of 147 *bHLH* protein-coding genes (Toledo-Ortiz et al.,

2003), which is a relatively high proportion relative to some other organisms (Riechmann et al., 2000). *bHLH* genes make up about 0.56% of transcription factors in Arabidopsis compared to 0.08% for *Saccharomyces cerevisiae*, 0.20% for *Caenorhabditis elegans* and 0.50% for *Mus musculus)*. Researchers have suggested that the expansion and diversification in number could be directly related to multicellularity implying that bHLH proteins are important regulators in cellular differentiation (Ledent et al., 2002; Toledo-Ortiz et al., 2003). Work in plants supports this hypothesis as bHLH proteins are master regulators of root epidermis differentiation (Bruex et al., 2012), stamen development, (Chen et al., 2016) cell elongation and division (Hao et al., 2012) and in the development of stomata (Lau and Bergmann, 2012; Pillitteri et al., 2007, 2011; Ran et al., 2013). Our lab has been historically interested in the role of bHLH proteins in the regulation of stomatal development and how they impact the production of these critical structures.

bHLH proteins in stomatal development

All land plants have epidermal structures called stomata that regulate the exchange of water vapor and gases between the plant and its environment (Chater et al., 2017; Peterson et al., 2010). In most dicotyledonous plants, stomata consist of two bean-shaped cells, called guard cells, surrounding a pore (Figure 1). The size of the pore is regulated by the turgor-driven movements of guard cells in response to environmental conditions, such as temperature, humidity, light intensity, the presence of pathogens (Ache et al., 2010; Elhaddad et al., 2014; Kostaki et al., 2020; Melotto et al., 2006). The production of stomata has become a model of cell-type differentiation in plants because the epidermis is easily accessible and epidermal cell types are highly distinguishable.

Beyond the ease of investigation, interest in stomata is tied to their impact on water use efficiency in plants. The genetic pathway by which cells differentiate from a non-descript protodermal cell into a stomata has been well-characterized over the past two decades (Balcerowicz and Hoecker, 2014; Kanaoka et al., 2008; Pillitteri et al., 2011; Richardson and Torii, 2013; Sugano et al., 2010; Wengier and Bergmann, 2012). These data have led to several studies indicating that reducing the number of stomata does not negatively impact photosynthetic capacity (Franks et al., 2015; Tanaka et al., 2013) and improves short- and long-term water use efficiency (Schlüter et al., 2003; Sugano et al., 2010; Yoo et al., 2011). These early studies imply that direct modification of stomatal density or development may provide an approach to impede the negative impacts on crops as global temperatures and drought increase.
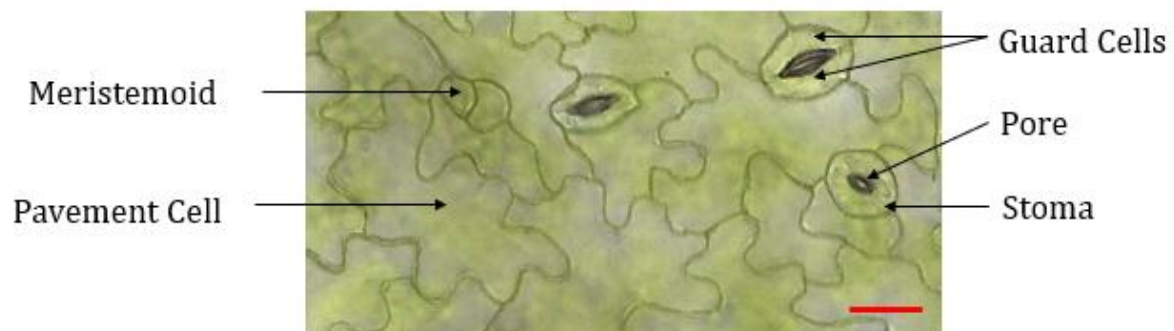
Figure 1. **Epidermal surface of an Arabidopsis leaf.** Light microcopy image of the abaxial leaf epidermis of an 8-week-old seedling. Guard cells, stoma, pore, meristemoid, and pavement cell are labeled. Cell walls are outlined using Microsoft Paint 3D. Scale bar = 50 µm.

Many types of proteins are known regulators of stomatal development and density. These include bHLH transcription factors, receptor kinases, MYB proteins and small secreted peptide ligands (Bergmann et al., 2004; Han et al., 2018; Hara et al., 2007; Lai et al., 2005; Lampard et al., 2008; MacAlister et al., 2007; Shpak et al., 2005; Tamnanloo et al., 2018; Zhang et al., 2015). The importance of bHLH proteins in this process is highlighted by the discoveries of five bHLH family members, SCREAM1/INDUCER OF CBF1 (SCRM1/ICE1), SCREAM2 (SCRM2), SPEECHLESS (SPCH), MUTE, and FAMA, that control the cellular transitions from protodermal cell to mature guard cell (Figure 2) (Kanaoka et al., 2008; MacAlister and Bergmann, 2011; Ohashi-Ito and Bergmann, 2006; Pillitteri et al., 2007). The conserved function of many these bHLH proteins can be traced across lineages and back to early land plants (Edwards et al., 1998; Ishizaki, 2017; Liu et al., 2009; Ortega et al., 2019; Wu et al., 2019).

Stomata develop from the outer most layer of the meristem, called the protoderm, which gives rise to several different cell types (Figure 2). In Arabidopsis, the epidermis contains three mature cell types: trichomes (hair cells), stomata guard cells, and pavement cells. When a protodermal cell enters the stomatal lineage (Figure 2), it transitions to a meristemoid mother cell (MMC), through mechanisms that are not clearly understood. The MMC undergoes an asymmetric entry division to create a small triangular cell called a meristemoid, which will eventually divide to produce the stomatal guard cells. The larger cell produced from the entry division is called a stomatal lineage ground cell (SLGC) and can either adopt pavement cell characteristics (Shpak et al., 2005) or it can undergo another round of asymmetric cell division, giving rise to another meristemoid. This asymmetric division of the MMC to produce a meristemoid requires the presence of the

bHLH protein SPCH. Meristemoids have stem-cell like properties and may continue to

undergo a variable number of amplifying divisions, up to three. The bHLH protein, MUTE,

is required to terminate meristemoid asymmetric divisions and allow transition into a

guard mother cell (GMC). The FAMA protein partly controls the final stage of stomatal

development, the symmetric division of a GMC and the differentiation of the daughter cells

into bean-shaped guard cells (GC) that flank the open pore (Larkin et al., 1997; Ohashi-Ito

and Bergmann, 2006; Zoulias et al., 2018).
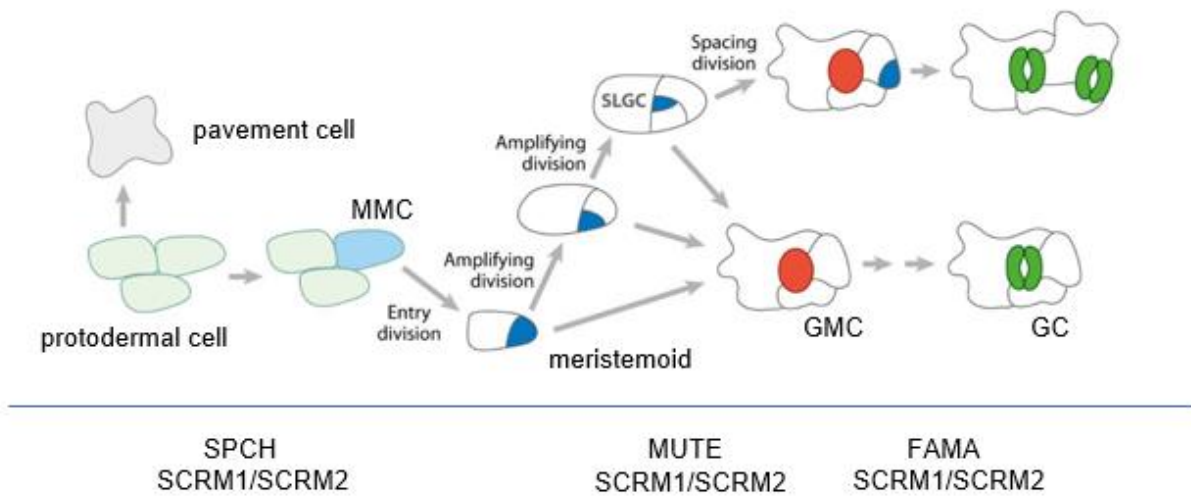
Figure 2. **Diagram of the cell types produced during stomata production in Arabidopsis**. The lineage begins with a protodermal cell (light green) that can become a pavement cell or enter the stomatal lineage by becoming meristemoid mother cell (MMC, light blue). MMCs can undergo an asymmetric entry division that produces a meristemoid (dark blue) and a stomatal-lineage ground cell (SLGC). SLGCs can differentiate into pavement cells or undergo an additional division to produce another meristemoid (spacing division). All meristemoids undergo a limited number of asymmetric amplifying divisions before they transition to a guard mother cell (red, GMC). The GMC divides symmetrically into two guard cells (dark green, GC) which form the mature stoma. The bHLH proteins that regulate the transition of cell types are indicated below the diagram in the place where they act. SPCH initiates the differentiation to MMC, MUTE terminates amplifying divisions and promotes the transition to GMC, and FAMA controls the transition of a GMC to a pair of GCs. SCRM and SCMR2 must be present throughout as a dimerization partner for SPCH, MUTE and FAMA. Modified from Pillitteri et al., 2007 (Pillitteri et al., 2007).

Two additional bHLH proteins are fundamental to the regulatory network of the stomatal lineage, SCRM1 and SCRM2 (Kanaoka et al., 2008). These proteins must be present at all stages of the stomatal pathway and are necessary for the cell-state transitions to occur. SCRM1 and its paralog SCRM2 are broadly expressed throughout all cell types of the stomatal lineage and form heterodimers with the transiently expressed SPCH, MUTE, and FAMA at the transition points of stomatal development (Kanaoka et al., 2008) (Figure 2).

Because bHLH proteins can only bind DNA as a dimer, studies have been performed to investigate potential interaction partners (Kanaoka et al., 2008; Lau and Bergmann, 2012; Lau et al., 2014; Ohashi-Ito and Bergmann, 2006; Putarjunan et al., 2019). The formation of the heterodimers between SCRM1 and SPCH, MUTE, and FAMA is critical to the progress of cell-state transition in the stomatal lineage (Kanaoka et al., 2008; Putarjunan et al., 2019). Bimolecular Fluorescence Complementation (BiFC) showed a strong interaction between FAMA and an additional family member, bHLH093, establishing protein-protein interaction between the two proteins *in planta* (Ohashi-Ito and Bergmann, 2006). Our interest in investing the role of bHLH093 in stomatal development rested in the documented interactions of this protein with an established stomatal regulator and its close phylogenetic relationship with both SCRM1 and SCRM2. Since the initiation of this project, bHLH093 has been named NO FLOWERING IN SHORT DAY (NFL) and along with its paralog bHLH061 have been shown to be involved in light sensing and meristem function (Poirier et al., 2018; Sharma et al., 2016)).

bHLH061 and bHLH093 as potential regulators of stomatal development

The evolutionary relatedness of the Arabidopsis bHLH family has been established

elsewhere (Heim et al., 2003; Toledo-Ortiz et al., 2003). The bHLH proteins, bHLH093/NFL

(At5g65640) and bHLH061 (At5g10570), are paralogs and members of the IIIb subgroup

based on (Heim et al., 2003) evolutionary relatedness and conserved amino acid motifs

outside of the DNA binding domain. The IIIb subgroup consists of four genes, *bHLH061*,

bHLH093, *SCRM1* (*bHLH116*, At3g26744) and *SCRM2* (*bHLH033*, At1g12860) (Table 1).

Table 1. **Members of the Arabidopsis bHLH-family subdivision IIIb***

bHLH number	Locus number	Gene Name and reference
bHLH093	At5g65640	*NFL* (Poirier et al., 2018; Sharma et al., 2016)
bHLH061	At5g10570	
bHLH116	At3g26744	*SCRM1/ICE1* (Chinnusamy et al., 2003; Kanaoka et al., 2008)
bHLH033	At1g12860	*SCRM2* (Kanaoka et al., 2008)

* Based on phylogenic evaluation (Heim et al., 2003)

Although the subgroup members are evolutionarily closely related, previous

investigation of the loss-of-function phenotype of *bHLH093* did not show any obvious

defects in stomatal formation similar to those observed for *SCRM1* (Kanaoka et al., 2008;

Poirier et al., 2018). However, lines ectopically overexpressing bHLH093 produced an

inconsistent weak phenotype similar to *fama* mutants (Ohashi-Ito and Bergmann, 2007),

producing occasional errors in GC production. Additional evidence for a potential role for

bHLH093 in stomatal development was from unpublished results from the Pillitteri lab that

indicated bHLH093 binds with MUTE in a yeast two-hybrid assay. The large expansion of

bHLH proteins in Arabidopsis was produced from a major duplication event, which can

often result in genetic and functional redundancy in the duplicated genes (Toledo-Ortiz et al., 2003). Overall, bHLH093 has 65% amino acid identity with bHLH061 (Figure 3). The sequence similarity between bHLH061 and bHLH093, their placement in subgroup IIIb with SCRM1and SCRM2, and that bHLH093 was shown to associate with MUTE and FAMA led us to the question of whether bHLH061 and bHLH093 are involved in stomatal development or some other developmental process.

```
bHLH061    --------METELTQLRKQ--ESN--NLNGVNGGFM-AIDQFVPNDWNFDYLCFNNLLQE      47
bHLH093    MELSTQMNVFEELLVPTKQETTDNNINNLSFNGGFDHHHHQFFPNGYNIDYLCFNNEEED      60
               :   **      **    .*  *  ..****     .**.**.:*:*******  ::

bHLH061    DDNIDHPSSSSLMNLISQPPPLLHQPPQPSSPL----YDSPPLSSAFDYPFLED---IIH     100
bHLH093    ENTLLY--PSSFMDLISQPPPLLLHQPPPLQPLSPPLSSSATAGATFDYPFLEALQEIID     118
           ::.: :   **:*:*********** : * *.**      .*   .::*******   **.

bHLH061    SSYSPPPLILPASQENTNN------YSPLMEESK--SF--ISIGETNKKRSNKKLEGQPSK     151
bHLH093    SSSSSPPLILQNGQEENFNNPMSYPSPLMESDQSKSFSVGYCGGETNKKKSKKLEGQPSK     178
           ** * *****  .**:. *        *****..:  **      *  .:*:..*********

bHLH061    NLMAERRRKRLNDRLSLLRSIVPKITKMDRTSILGDAIDYMKELLDKINKLQEDEQELG     211
bHLH093    NLMAERRRKRLNDRLSMLRSIVPKISKMDRTSILGDAIDYMKELLDKINKLQDEEQELG     238
           ****************.********:************************:*****

bHLH061    SNSH---------LSTLITNESMVRNSLKFEVDQREVNTHIDICCPTKPGLVVSTVSTLE     262
bHLH093    NSNNSHHSKLFGDLKDLNANEPLVRNSPKFEIDRRDEDTRVDICCSPKPGLLLSTVNTLE     298
           ...:        *. * :** :**** ***:*:*: :*::****  ****::***.***

bHLH061    TLGLEIEQCVISCFSDFSLQASCFEVGEQRYMVTSEATKQALIRNAGYGGRCL     315
bHLH093    TLGLEIEQCVISCFSDFSLQASCSEGAEQRDFITSEDIKQALFRNAGYGGSCL     351
           *********************** * .*** ::*** ****:******* **
```

Figure 3. **Amino acid sequence alignment of Arabidopsis bHLH093 and its paralog bHLH061.** Sequence alignment generated with Clustal Omega showing high amino acid identity (asterisks) between bHLH093 and bHLH061 both within and outside the bHLH domain. Sequences were obtained from TAIR (https://www.arabidopsis.org). Solid red line indicates the basic region, red dashed line indicates the helix-loop-helix region.

Functional roles for bHLH061 and bHLH093 from recent literature

At the time this study was started, functional analysis of bHLH061 and bHLH093 had not been published. During our investigation, two peer-reviewed publications were

released that implicate bHLH093 and bHLH061 in the promotion of flower development under short-day conditions and in apical meristem function (Poirier et al., 2018; Sharma et al., 2016). These papers established that bHLH093 is nuclear-localized, expressed in several tissues of the plant, including shoot and root meristems, and that its function is dependent on both light intensity and photoperiod. Neither of these articles look at stomatal development in depth or postulated any role for either bHLH061 or bHLH093 in stomatal development. Because stomatal development requires careful cell counting and cell-identification, it has been overlooked or not investigated when looking at phenotypic changes (Kanaoka et al., 2008; Shpak et al., 2005).

Sharma et al. named *bHLH093 NO FLOWERING IN SHORT DAY* (*NFL*) based on its non-flowering phenotype under short days. In their study, plants were grown in short-day (SD) conditions, 8 hrs light and 16 hrs dark (Sharma et al., 2016). Due to the importance of flowering, it is controlled by a highly connected and complicated web of signaling pathways that incorporate temperature, time, environment, and photoperiod cues to determine correct floral timing and ensure reproductive success. Photoperiod refers to the day length, the number of hours that the plant is exposed to light during a 24 hr day cycle. Arabidopsis is a facultative long-day (LD) plant, meaning that LD conditions hasten flowering, but wild-type (WT) plants will eventually flower under SD conditions. Sharma et al., determined that under SD conditions, *nfl* plants never flowered (Sharma et al., 2016). *Nfl* mutants continued to grow vegetatively and had twice as many leaves as WT, a common means of measuring flowering time (Koornneef et al., 1991). Under LD conditions, 16 hrs light and 8 hrs dark, flowering time was not significantly different between *nfl* and WT plants. Gibberellic acid is an absolute requirement for flowering in Arabidopsis under SD conditions, where in the

absence of the other flowering signals GA directly promotes the activation of floral identity genes (Wilson et al., 1992; Yu et al., 2004). GA biosynthesis and metabolism are altered in *nlf* mutants compared to WT plants resulting in multiple developmental defects under SD (short stature, darker curled leaves, and no flowering). Sharma et al. found that the delay in flowering in the *nfl* mutant could be partially rescued by direct application of gibberellin. Overall, they concluded that NFL is a key regulator of flowering under SD conditions and that it functions upstream of GA to promote the expression of floral identity genes to induce flowering.

A more recent paper (Poirier et al., 2018) built on the work of Sharma et al. and investigated both bHLH061 and bHLH093 in development. They were able to confirm that these genes play a role in GA signaling. Specifically, Poirier et al., found that the absence of bHLH093 and bHLH061 results in structural defects in the apical meristem. They investigated the single mutants, *bhlh061* and *bhlh093*, as well as the double mutant *bhlh093/bhlh061* under LD conditions with varying light intensities. Low-medium light intensity (90-120 μmol m^{-2} s^{-1}) didn't produce differences in phenotype from WT. However, high light intensity (150-250 μmol m^{-2} s^{-1}) caused several growth defects in the double mutants compared to WT that implicated a disruption in GA signaling. Rosette leaf morphology was impacted, the leaves curled downwards, and their surface was rough. Inflorescence production was delayed, overall growth was impaired, and leaves continued to emerge for a much longer time than WT under high intensity light conditions. Poirier et al. did look at stomatal density (number of stomata in an area of leaf divided by that area) based on similar rationale as our lab. They did not find any difference in stomatal density

between *bhlh093/bhlh061* and WT and did not observe any clustering of stomata or aberrant cell divisions.

These papers clearly established that bHLH061 and bHLH093 play a role in maintaining the identity of the shoot apical meristem and that GA deficiency is responsible for the floral timing defects. Together, the recent published work proposes a model that bHLH061 and bHLH093 act upstream of GA signaling in the shoot meristem in a light/photoperiod dependent manner to regulate growth and promote flowering. The loss of these proteins in the double mutant decreases GA levels and perception, which disrupts tissue development and leads to a non-functional shoot apical meristem.

Further investigation of bHLH061 and bHLH093

Our investigation of bHLH061 and bHLH093 was initiated prior to any published data. Although the recent research on these two proteins have provided mechanistic insight into their roles during development, confirmation and repetition of published finding is a critical and important aspect of scientific discovery. Protein-protein interaction studies implicated bHLH093 as a binding partner for MUTE (Pillitteri lab, unpublished) and FAMA (Ohashi-Ito and Bergmann, 2007) which could lead to subtle changes in stomatal development. While Sharma et al. (Sharma et al., 2016) and Poirier et al. (Poirier et al., 2018) focused on the role of these two proteins in flowering and meristem function, we additionally focused our investigation on potentially subtle stomatal changes while also looking at flowering time and general growth parameters to contribute to published findings.

Methods

Plant material and growth conditions

The Columbia (Col) ecotype of *Arabidopsis thaliana* was used as the wild-type (WT) background for these experiments. All T-DNA insertion mutant seeds used in this study were obtained from the *Arabidopsis* Biological Resource Center (Alonso et al., 2003). The lines used were SAIL_569_E06/CS824212 for At5g10570, *bHLH061* and SALK_121082C for At5g65640, *bHLH093*. Seeds were surface sterilized for 10 minutes in 0.5-1 ml of a Triton X-100 and sodium hypochlorite solution (v/v 0.1% Triton X-100, 30% sodium hypochlorite) under constant motion on a nutating mixer (Fisher Scientific, Fair Lawn, NJ). Seeds were rinsed at least 4 times in sterile water under aseptic conditions and kept at 4 °C for at least 24 hours. Seeds were plated onto 0.5X Murashige and Skoog medium (Caisson Labs, Logan UT) supplemented with 1X with Gamborg's Vitamin Solution (Caisson Labs, Logan, UT). Briefly, 2.17g MS salts and 10 g glucose were dissolved in 900 ml H_2O, pH was adjusted to 5.7 with 1M potassium hydroxide (KOH), 8.5 g agar was added (Fisher Scientific), and the solution was brought to volume for 1l. After autoclaving 1ml of 1000X Gamborg's Vitamin Solution was added. If needed, antibiotics were added for a final concentration of 50 μg/ml for kanamycin and hygromycin, and 100 μg/μl for Timentin. Seed sowing was done under aseptic conditions in a laminar flow hood and plates were sealed with 3M Micropore™ tape (3M, St Paul, MN). Plants were transferred to soil at approximately 16 days after germination. The soil mix was a 2:1:1 ratio of peat soil, vermiculite, and perlite. Approximately 6 pellets of slow-release fertilizer (Osmocote

Smart-Release® Plant Food, Marysville, OH) were added per pot. Growth conditions for all plants at all stages were 22-24 °C with a 16 hr light/8 hr dark cycle (Long-day cycle). Light intensity during growth was between 90-120 µmol m^{-2} s^{-1}.

DNA extraction

DNA was extracted via isopropanol precipitation. Leaf material of approximately 15 mm^2 was ground up in 150 µl of DNA extraction solution (200 mM Tris-HCl at pH=7.5, 250 mM NaCl, 25 mM EDTA, 0.5% SDS) using a sterile plastic pestle then centrifuged 5 min at 13000 rpm at 10°C. DNA was precipitated by combining 150 µl of supernatant to 150 µl of isopropanol. Tubes were quickly inverted several times and centrifuged 5 min at 13000 rpm at room temperature. The supernatant was discarded, and the pellet was rinsed with approximately 500 µl of 70% EtOH. Tubes were inverted on kim-wipes and allowed to dry at room temperature for at least 30 minutes. The pellet was resuspended in 50 µl of sterile Millipore-filtered water and used immediately or stored at -20 °C until use.

Primers

All primers were obtained from Eurofins mwg/operon (Huntsville, AL) and resuspended in sterile water to 10 µM. Names, sequence, and melting temperature (T$_m$) of primers used in this study are given in Table 2 and Table 3.

Table 2. **Sequence of gene-specific primers**. Primers used for amplification of coding regions for construction of overexpression constructs and to assess transcript presence/absence by Reverse-Transcription Polymerase Chain reaction (RT-PCR). Actin primers were used as a positive control.

Gene locus and name	Primer name	Primer Sequence (5' to 3')	T_m (°C)
At5g10570 *bHLH061*	bHLH061_-1838.GW	CACCATTATGGGCCTTTATCTAATCG	63
	bHLH061_1.GW	CACCATGGAAACGGGAATTCACGC	64.6
	bHLH061_1523.rc	CAGACATCTTCCTCCATAAC	58.4
	bHLH061_1526.rc	CTACAGACATCTCCTCCATAAC	61
	bHLH061_504	GTTAAATGACCGACTCTCC	58
At5g65640 *bHLH093*	bHLH093_-2475.GW	CACCCGCATATCATAGCTTCTCATG	64.6
	bHLH093_1.GW	CACCATGGAACTGTCGACTCAATG	64.6
	bHLH093_1765.rc	CAAGCATGCTTCCACCATAACCTG	64.6
	bHLH093_1768.rc	TTACAAGCAGCTTCCACCATA	58.7
Actin	ACT 2-1	GCCATCCAAGCTGTTCTCTC	62.4
	ACT 2-2	GCTCGTAGTCAACAGCAACAA	60.6

Table 3. **Sequence of genotyping and insert verification primers**. Primers used in combination with gene-specific primers to determine the allele state of T-DNA insertion sites for bHLH061 and bHLH093 and for insert verification in pLB lines.

Gene or T-DNA insertion line	Primer name	Primer Sequence (5' to 3')	T_m (°C)
CS824212	SAIL LB3	TAGCATCTGAATTTCATAACCAATCTCGATACAC	64.7
SALK_121082	LBA1	TGGTTCACGTAGTGGGCCATCG	61.5
35S promoter	GWB235S	CACCCCTGCAGGTCAACATGGTGGAGC	66.8

Vector Construction

Vectors produced in this study were done using the Gateway™ cloning system

(Invitrogen, Carlsbad, CA). For 35S Cauliflower Mosaic Virus (CaMV) ectopic

overexpression, primers were designed to amplify the entire coding sequence including the

STOP codon. All forward primers contained a TOPO entry vector (Invitrogen) sequence (CACC) at the 5' end for directional cloning based on manufacturer's instructions for directional cloning into TOPO-D/pENTR vector.

Full-length gene sequences for *bHLH061* and *bHLH093* were amplified from WT genomic DNA via end-point polymerase chain reaction (PCR). The following reagents were used in a 20ul total volume PCR reaction; 2 μl of 5X Phusion HF buffer, 10 mM dNTPs for 200 μM final concentration, 10 μM of forward and reverse primers, and 0.2 μl /0.4U of Phusion® High-Fidelity DNA Polymerase (New England BioLabs, Ipswich, MA). All reactions were set up on ice with 3 μl of WT genomic DNA as template at variable concentrations. Reactions were run in a thermal cycler (Applied BioSystems 2720) using the following parameters: 1 min at 98 °C ; 30 cycles of: 10 s at 98 °C, 30s at 53 °C, 1min/kbp at 72 °C, followed by a final elongation for 5 min at 72 °C.

Amplification products (18 μL of reaction + 1μL of loading dye) were loaded and run on a 1.0% (w/v) TAE (Tris-Acetate-EDTA) agarose gel with ethidium bromide (0.5μg/mL) at approximately 100V for 60 minutes and individual bands were excised from the gel under UV light and placed in a 1.5 ml tube. PCR products were gel purified using an UltraClean® 15 DNA Purification Kit (Mo Bio Laboratories Inc, Carlsbad, CA) according to the manufacturer's directions.

Construct names, primers, and predicted amplicon size (insert size) for each construct are given. WT Col DNA was used as DNA source for amplicon production.

Table 4. **Gateway cloning Entry vector detail**

Name	BaseVector	Insert	Insert size	Primers used for insert amplification	
				Forward	Reverse
pLB100	pENTR™	*bHLH061* coding sequence	1526 bp	bHLH061_1.GW	bHLH061_1526.rc
pLB102	pENTR™	*bHLH093* coding sequence	1768 bp	bHLH093_1.GW	bHLH093_1768.rc

Directional cloning via TOPO®

Gel-purified DNA amplification products were ligated into a pENTR entry vector using the pENTR™ Directional TOPO® Cloning Kit (Invitrogen/Life Technologies/ThermoFisher Scientific, Waltham, MA) using the instructions supplied by the manufacturer producing pLB100 and pLB102 (Table 4). The resulting product was then used to transform chemically competent One Shot TOP10 *Escherichia coli* using a standard heat-shock method.

Briefly, 2 µl of TOPO reaction product was added to 50 µl of chemically competent cells, One Shot® TOP10 strain (ThermoFisher Scientific, Waltham, MA) or DH5α strain. Cells were incubated on ice for 5 minutes, placed in a dry block for 30 s at 42 °C, and immediately placed back on ice. 950 µl of SOC medium (2% w/v Bacto™ Tryptone (BD, Sparks, MD), 5% w/v yeast extract (Fisher Scientific, Fair Lawn NJ), 8.6 mM NaCl (Sigma-Aldrich, St Louis MO), 2.5 mM KCl (Fisher Scientific), 1 µl each of 2M Mg^{2+} and 2M Glucose was added to each transformation reaction. The transformation reactions were placed horizontally on an orbital shaker at 225 rpm and 37 °C for one hour. The transformation reactions were centrifuged at 8000 rpm for one minute, and 800 µl of supernatant were removed. The pellet was resuspended in the remaining 200 µl of SOC medium. The

manufacturer's directions were used in the case of the One Shot® TOP10 cells. To select

transformants, 100 μl of transformation reaction was spread onto Luria-Bertani (LB)

media (Fisher Scientific) and kanamycin at a final concentration of 50 μg/ml. Plates were

incubated at 37 °C overnight and positive transformants were verified via PCR.

Ectopic overexpression vector construction

The 35S CaMV ectopic overexpression vectors (Table 5) were created using the

Gateway® LR Clonase® II kit (ThermoFisher Scientific, Waltham, MA) following the

manufacturer's instructions. The destination vector was the Gateway® binary vector

pGWB2 (Nakagawa et al., 2007) which carries the cauliflower mosaic virus (CaMV) 35S

constitutive promotor upstream of the LR recombination sites. This vector confers both

kanamycin and hygromycin resistance (Table 6). 2μL (approximately 100ng) of pLB100 or

pLB102 and 2μL (approximately 150 ng) of pGWB2 (Nakagawa et al., 2007) were

combined together with 2μL of Gateway LR Clonase II (Invitrogen) and TE buffer (100mM

Tris-HCl and 10mM EDTA (pH 8.0) to a total volume of 10μL. Reactions were incubated for

2 hours at 25°C. Following incubation, 1μL of Proteinase K solution (2μg) was added and

further incubated at 37°C for 10 minutes. Plasmid concentrations of vectors were

determined using a NanoDrop™ spectrophotometer (ThermoFisher Scientific).

Table 5 **CaMV ectopic overexpression vector detail**

Construct name	Destination vector	Entry vector	Vector Description
pLB104	pGWB2	pLB100	CaMV35S:: At5g10570/*bHLH061* coding sequence bHLH061
pLB102	pGWB2	pLB102	CaMV35S:: At5g65640/*bHLH093* coding sequence bHLH093

Table 6. **35S CaMV Destination vector (GWB2) detail**

Vector name	Bacterial selection	Gateway cassette	Plant selection	Description	Accession Number
pGWB2	Km^r, Hyg^r	P$_{35S}$-*att*R1-Cm^r-*ccd*B-*att*R2-T$_{NOS}$	NPTII (Km^r) HPT (Hyg^r)	35S CaMV promoter upstream of cloning site	AB289765

Data from Department of Molecular and Functional Genomics, Interdisciplinary Center for Science Research, Organization for Research and Academic Information, Shimane University. Km, kanamycin; Hyg, hygromycin.

4 µl of Clonase™ reaction was used to transform DH5α *E. coli* according to the protocol described above with one modification: the bacteria were placed in a dry block at 42 °C for 45 seconds for heat shock. Transformation reactions were spread onto plates with kanamycin and hygromycin at 50ug/ml each. A master plate was created from select colonies and an overnight culture of LB and selecting antibiotics at 50 µg/ml was inoculated. The cultures were placed in a shaking incubator at 225 rpm and allowed to grow overnight at 37 °C. After 12-18 hours, the plasmids were purified using a Qiagen QIAprep Miniprep as described previously. The presence of the gene in this plasmid was verified using PCR. The PCR reaction parameters were as described above.

Construct Verification

Initial verification of pLB100 and pLB102 or pLB104 and pLB106 transformants was done using end-point PCR (Table 7). A 5ml overnight culture (LB, kanamycin) was grown and pure plasmid was isolated using a Qiagen QIAprep Miniprep (Qiagen). Verification of transformants was done using end-point PCR. PCR reactions were performed in a total volume of 20 µl with 0.5 µl of purified plasmid DNA or small amount of colony as template. Reactions were performed using 0.5 µl EX Taq DNA polymerase (Takara Bio Inc, Mountain View, CA), 2 µl 10X EX Taq buffer, 1 µl dNTP mix, 0.5 µl each of primer for a final concentration of 200 µM. Reactions were run in a thermal cycler (Applied BioSystems 2720) using the following parameters: 1 min at 98 °C; 30 cycles of: 10 s at 98 °C, 30 s at 55 °C, 3min30s at 72 °C, followed by a final elongation for 5 min at 72 °C. Entry vector insert sequences were confirmed by Sanger sequencing (McLAB, San Francisco, CA). Long-term storage glycerol stocks were created by combining 750 µl of overnight culture with 750 µl of 80% glycerol and frozen in cryotubes at -80 °C.

Table 7. **Primers pairs used for insert verification.** Primer pairs used for Entry vector (pLB100 and pLB101) and CaMV35S ectopic overexpression vector (pLB104 and pLB106) verification.

	Construct	Forward Primer	Reverse Primer
At5g10570	pLB100	bHLH061_1.GW	bHLH061_1526.rc
At5g65640	pLB102	bHLH093_1.GW	bHLH093_1768.rc
At5g10570	pLB104	GWB235S	bHLH061_1526.rc
At5g65640	pLB106	GWB235S	bHLH093_1768.rc

***Agrobacterium tumefaciens* transformation**

Agrobacterium tumefaciens, was transformed via electroporation using a BioRad Gene Pulser II system (BioRad, Hercules, CA) with the following parameters: 0.5 µl of purified plasmids pLB104 or pLB106 were added to 50 µl of GV3101 electrocompetent *Agrobacteri*a. The BioRad Gene Pulser II was set to the following parameters: resistance 200 Ω, voltage 1.8 V, capacitance 25 µF. After electroporation, 1 ml of ice cold SOC was added, and the transformation reactions were shaken horizontally on an orbital shaker at 30 °C for 1 hour at 225 rpm. 50 µl of the transformation reaction was then spread on LB media with selecting antibiotics and grown for 2 days at 30 °C.

Overnight cultures were made from positive transformants and plasmid purification was performed using the Qiagen MiniPrep kit with the following modification to the manufacturer's protocol: 350 µl of resuspension buffer, 350 µl extraction/lysis buffer, and 450 µl of neutralization buffer. Glycerol stocks were made and stored as described.

Arabidopsis Transformation

Transformation of WT plants was done by Agrobacterium-mediated transformation using floral dip method (Clough and Bent, 1998) Briefly, Agrobacteria carrying either pLB104 or pLB106 (Table 5) were used to inoculate 5 ml LB with kanamycin (50 µg/ml) and hygromycin (50 µg/ml) and grown for 16 hours at 30°C at 225rpm. A 1 ml aliquot was removed to inoculate a 250 ml culture and incubated for an additional 16 hours at 30°C at 225rpm. Individual cultures were transferred to 250 ml centrifuge tubes and centrifuged at 5200 rpm for 20 minutes at 4°C. The supernatant was removed, and the pellet was gently resuspended in transformation solution (5% sucrose, 1X Gamborg's vitamins (Caisson

Smithfield UT), 50 µl/l Silwet L-77 (Lehle Seeds Round Rock TX). Inflorescences, or in some cases whole plants, were dipped into the transformation solution for 30 seconds with gentle swirling. The plants were placed upright and tented in plastic wrap to maintain high humidity conditions for 24 hours at room temperature before being moved to standard growth conditions and watered as needed.

Transgenic seedling selection

T1 seeds were collected in bulk from *Agrobacterium*-infiltrated WT (T0) plants and stored at room temperature in labeled 1.5ml tubes. Between 1000-1500 T1 seeds were surface sterilized as previously described and sowed directly onto 0.5X MS selective media containing kanamycin (50µg/mL), timentin (100mg/mL), and hygromycin (50µg/mL). Seeds were evenly dispersed on the plates using a 0.1% (w/v) agar solution. Each plate was sealed with micropore tape (3M Healthcare), placed at 4°C for at least 24 hours and transferred to standard growth conditions. Positive transformants (T1 seedlings) that were resistant as determined by strong root development and green color were transplanted to soil, verified via PCR for the appropriate insert and their T2 seed were collected from individual T1 plants. Between two and five T1 lines were collected for each construct. Approximately 100 T2 seeds from independent T1 lines were surface sterilized and germinated on MS media with kanamycin (50µg/mL) and hygromycin (50µg/mL). A subset of selected T2 seedling populations that displayed resistance at a ratio of ~3:1 were transplanted onto soil for collection of next generation seed (T3). Approximately 100 seeds from individual T3 plants from each line were plated onto antibiotic selective MS media and scored for segregation and resistance; seed populations that did not produce

susceptible plants in the T3 generation were collected and stored as a homozygous line. PCR confirmation was conducted on all collected T3 individuals to confirm insertion of the transgene.

Loss-of-function mutant verification

Independent T-DNA insertion lines of bHLH061 and bHLH093 (Table 8) were purchased from ABRC for evaluation. Seeds were sterilized, plated, and transplanted as described above. DNA extraction and PCR were performed using gene-specific primers (Table 8) in combination with T-DNA border primers (Table 3) to determine the presence of the T-DNA insert in single and double loss-of-function mutants.

Table 8. **T-DNA insertion lines evaluated in this study.**

		Primers	
Gene locus/name	Insertion line	Gene-specific primer	T-DNA border primer
At5g10570/*bHLH061*	CS 824212	bHLH061_1.GW	SAIL LB3
At5365640/*bHLH093*	SALK_121082	bHLH093_1.GW	LBA1

Plant height evaluation

Plant height was determined for individual WT, bHLH061 ox, bHLH093 ox, *bhlh061*, *bhlh093* plants and double knockout plants from the base of the rosette to the tip of the longest inflorescence. Measurement were made at the end of development/start of senescence (siliques started to shatter and brown) (Boyes et al., 2001) using a standard ruler. Plants were grown at 6 plants/pot for this evaluation.

Root length evaluation

Root length was determined for WT, bHLH061 ox, bHLH093 ox, *bhlh061*, *bhlh093*
plants, and double knockout plants. Seeds of each line were sterilized and stored at 4 °C for
at least 24 hours, then sowed in a horizontal line on 0.5X MS plates with no selecting
antibiotics. Plants were grown under standard conditions detailed above. The plates were
supported at a 70-degree angle (20 degrees from vertical) to simulate downward growth
on the surface of the media. The root length of the seedlings was evaluated at 10 days after
plating using a ruler, either from measuring on the plate or removing the seeding from the
plate and measuring directly. The two methods did not yield statistically different results.

Floral timing evaluation

Flowering time was defined at the number of days past germination that the first
flower was observed (Koornneef et al., 1991) . The date of the flowering was recorded, the
plant was removed from the pot and the true leaves of the rosette were removed and
counted in destructive sampling (Koornneef et al., 1991). This experiment was carried out
for bHLH061 ox and bHLH093 ox overexpressing lines (T4 generation), for *bhlh061* and
bhlh093 (the single knock outs CS 824212 and SALK 121082), and double knockout lines.

Stomata evaluation

Images of the abaxial leaf epidermal surface was used for all stomatal analyses. All
images were taken using a Leica DM 750 Microscope with a ICC50HD camera and the Leica
Application Suite (LAS EZ, version 3.0.0, Leica Microsystems, Switzerland) processing
software. Individual true leaves from approximately 21-day old *A. thaliana* seedlings were

removed from individual plants and mounted in deionized water on a standard slide with coverslip. Ideally, 10 images from 10 different seedlings were taken, though some observations were from different leaves on the same plant. Seedlings from the CaMV35S ectopic overexpression lines, bHLH061 ox and bHLH093 ox, single mutant SALK lines *bHLH061* (SAIL_569_E06 / CS824212 for At5g10570) and *bHLH093* (SALK_121082C for At5g65640), the F3 and F4 generation of double mutant lines, and Columbia ecotype (WT) control were investigated. Images were loaded in the GIMP (GNU Image Manipulation Program). The number of pavement cells, stomata, and meristemoid cells were counted (Figure 1). The number of each cell type was documented and calculated for each plant type using the following equation.

$$Stomatal\ index\ (SI) = \frac{Number\ of\ stomata}{Number\ of\ pavement\ cells + Number\ of\ stomata}$$

Significance for all measurements was determined using a two-tailed Student's t-test (p-value of 0.05 as significance minimum) with Bonferroni correction for multiple comparisons. Stomatal irregularities (single guard cells, stomata doubles or clusters) were documented from visual observation.

RNA isolation and Reverse- transcription PCR (RT-PCR)

Total RNA was extracted from WT, CaMV35S ectopic overexpression lines (pLB104 and pLB106), mutant lines (CS824212 and SALK_121082) and the double knockout mutant of *Arabidopsis thaliana.* Total RNA was extracted from approximately 5 10-day old

seedlings using the Qiagen RNeasy Plant Mini Kit (Qiagen, Valencia, CA) with on-column

DNAse treatment following manufacturer's instructions. The RNA was eluted into 42 μl of

H_2O. RNA purity and yield were confirmed using a NanoDrop spectrophotometer.

The SuperScript™ III First Strand Synthesis System for RT-PCR (ThermoFisher Scientific)

was used to generate cDNA. 600 ng of RNA was used in each reverse transcriptase

reaction.2 μl of cDNA was used as template for a PCR with the appropriate primers.

showsthe primer pairs used for amplification as well as the expected size of the PCR

product. Amplification of the *ACT2* gene was used to verify equal loading of cDNA and RNA

integrity.

TaKaRa EX Taq DNA Polymerase (Takara Bio Inc, Mountain View, CA) was used as

the polymerase with the following volumes: 2 μl 10X EX Taq buffer, 1 μl dNTP mix, 0.5 μl

each of primer for a final concentration of 200 μM, and 0.5 μl EX Taq DNA polymerase.

Reactions were run in a thermal cycler (Applied BioSystems 2720) using the following

parameters: 1 min at 98 °C; 30 cycles of: 10 s at 98 °C, 30 s at 55 °C, 3min30s at 72 °C,

followed by a final elongation for 5 min at 72 °C. The PCR products were run out on a 1%

agarose gel and relative band size and brightness was evaluated. Table 9 details the

primers pairs and the expected results.

Table 9. **Primer pairs and expected band size from RT-PCR**

Genotype	Forward primer	Reverse Primer	Band expected (Yes/No)	Expected result, bp
bHLH061 ox	bHLH061_504	bHLH061_1523.rc	Yes	460
bHLH093 ox	bHLH093_1.GW	bHLH093_1765.rc	Yes	1053
bhlh061	bHLH061_504	bHLH061_1523.rc	No	
bhlh093	bHLH093_1.GW	bHLH093_1765.rc	No	
bHLH093xbHLH061	bHLH061_504	bHLH061_1523.rc	No	
	bHLH093_1.GW	bHLH093_1765.rc	No	
	bHLH093_1.GW	bHLH093_1765.rc	No	
WT	bHLH061_504	bHLH061_1523.rc	Yes	460
WT	bHLH093_1.GW	bHLH093_1765.rc	Yes	1053
All genotypes	ACT 2-1	ACT 2-2	Yes	349

<center>**Results**</center>

***bHLH093* and *bHLH061* gene structure and expression**

Our initial investigation of bHLH061 and bHLH093 in stomatal development was founded in both published and unpublished work that demonstrated bHLH093 could directly interact with the bHLH proteins FAMA (Ohashi-Ito and Bergmann, 2006) and MUTE (Pillitteri, unpublished). In addition, bHLH061 and bHLH093 have high sequence identity to each other and SCRM1/SCRM2, which are known binding partners of SPCH, MUTE and FAMA (Kanaoka et al., 2008; Pillitteri et al., 2007). This suggested these proteins may be involved in stomatal development, but perhaps not exclusively involved in that process. Therefore, I sought to determine the potential functions of bHLH061 and bHLH093 through overexpression and mutant phenotype analysis across multiple developmental traits.

bHLH061 and bHLH093 share significant sequence identity and gene structure (Figure 4, Figure 5). Long-standing work has demonstrated that the amino acid positions 5-9-13 within the basic region of the bHLH domain are critical for DNA binding. All non-plant and most plant bHLH proteins have a His-Glu-Arg (H-E-R) in those positions and bind the canonical E-box, CANNTG (Figure 4). All members of subgroup IIIb have an Asp-Glu-Arg (N-E-R), suggesting a possible lack of DNA binding. However, Chinnusamy et al. (Chinnusamy et al., 2003) clearly demonstrated that SCRM1 binds specifically to the consensus sequence CATTCG of the C-REPEAT BINDING FACTOR3 (CBF3) promoter. Therefore, it is likely that all members are capable of DNA binding and functioning as transcriptional regulators. In

<center>30</center>

addition, the conserved Leu at position 23 (helix 1) and 49 (helix 2) are highly conserved among dimerizing bHLH proteins and generally necessary for dimerization to occur (Heim et al., 2003)(Figure 4). All members of subgroup IIIb have these conserved dimerization residues, which implies that bHLH061 and bHLH093 also function as dimers similar to the other subgroup members (Figure 4).

The bHLH061 protein product is 315 amino acids in length and the gene length is 1526 base pairs from the ATG start codon to the TAG stop codon. Intron-exon structure is the same in all IIIb members consisting of four exons and three introns (Figure 5a). The distance to the closest upstream gene is 2005 base pairs. *bHLH093* is 1768 bp long from start to stop codon (Figure 5b) which codes for a 351 amino acid protein. The distance to its nearest upstream gene is 8879 base pairs. Intervening regions between genes in Arabidopsis can be as small as 200 base pairs, therefore the size of the upstream noncoding region for both *bHLH061* and *bHLH093* is comparatively large, which could imply the need for extensive regulatory sequences. The experimental investigation regulatory sequences, functional promoter length, and expression pattern of bHLH061 or bHLH093 was out of the scope of this study. However, based on publicly available data and published results, using a promoter of approximately 2000 bp, bHLH093 was expressed strongly in meristems, leaves, and roots (Poirier et al., 2018; Sharma et al., 2016). The expression pattern of bHLH061 has not been published and is not defined well in publicly available data because it was not present on the original Arabidopsis ATH1 GeneChip. However, more recent RNA-seq work suggests it is highly expressed in mature leaves. Based on available data, bHLH061 and bHLH093 do not have a strong transcriptional response to either hormone or abiotic stress treatments.

Confirmation of increase in transcript abundance in bHLH061 ox and bHLH093 ox

Overexpression of gene products is a common way to gain insight into the potential role of a gene in developmental processes. The most commonly used overexpression promoter in Arabidopsi*s* is the 35S Cauliflower Mosaic Virus (CaMV) promoter. This promoter has strong, constitutive expression in most organs in Arabidopsis (Benfey and Chua, 1990). Although natural plant promoters with constitutive activity have been used to ectopically overexpress genes, the activity of these promoters tends to be affected by endogenous plant signals, sometimes resulting in undesired or unanticipated activity (Amack and Antunes, 2020; Napoli et al., 1990).

Despite the potential for gene repression due to high overexpression of transcripts, the CaMV promoter has been pivotal and the most well-studied means of gene overexpression in plants (Amack and Antunes, 2020). To this end, I produced transgenic plants that contain the CaMV promoter driving the expression of the open reading frame of either *bHLH061* (bHLH061 ox) or *bHLH093* (bHLH093 ox), which consisted of the full genomic sequence including the start and stop codons.

Approximately 8 independently transformed lines were isolated for both bHLH061 ox and bHLH093 ox. Initial identification of single-insert, homozygous lines were determined by antibiotic-resistance segregation ratios. Subsequently, I confirmed that homozygous lines produced higher levels of *bHLH093* or *bHLH061* mRNA transcripts compared to WT using RT-PCR qualitative comparison. Total RNA was isolated, and first stand cDNA was produced from WT and individual T4 generation from both bHLH061 ox and bHLH093 ox plants. bHLH061 ox and bHLH093 ox produced a clear qualitative

increase in mature transcript levels in CaMV overexpression lines compared to WT (Figure 6). In addition to the mature transcript size for each gene (Figure 6, yellow arrow), I observed several larger-sized amplification products that only appeared in the overexpression lines. These may represent alternate or mis-spliced transcripts produced based on ectopic overexpression, but they were not sequenced to determine their likely origin. I did not investigate the corresponding protein levels in either bHLH061 ox or bHLH093 ox. However, the correlation between mRNA and protein abundance in a wide range of organisms is generally considered to be positive, although not universal (Abreu et al., 2009; Plotkin, 2010; Vogel and Marcotte, 2012). All phenotypic analysis was done using a bHLH093 ox and bHLH061 ox line confirmed to have an increase in transcript abundance.

Characterization of bHLH061 ox and bHLH093 ox phenotypes

Although I was interested in the role that bHLH061 and bHLH093 may play in stomatal development based on their association with known stomatal regulators, I did not limit myself to this developmental process. To this end, I also investigated several developmental categories outside of stomatal development.

Plant height

I evaluated height at the start of senescence when siliques started to turn brown and shatter. All genotypes were around 260mm tall with little variance among individual plants. Final plant height was not different between WT and bHLH061 ox or bHLH093 ox (Figure 7).

Root length

Based on data implicating bHLH093 expression in roots (Sharma et al., 2016) (TAIR, https://www.arabidopsis.org), I investigated root length to determine if below ground organs were impacted by bHLH061 ox and bHLH093 ox. To measure root length, I used a standard method (Furner, 1992) of germinating seeds on media plates placed on an incline. The offset from horizontal position results in root growth on the surface of the media and allows for measurement with minimal manipulation (Figure 8). The root length data were averaged from at least 28 of individual plants for each overexpression line and 10 for WT. Average root lengths for bHLH061 ox was significantly different from WT (23.7mm vs 16.6 mm; $p = 0.01$). In contrast, bHLH093 ox had similar average root lengths to WT (17.9 mm vs 16.6 mm; $p = 0.55$) (Figure 9 and Table 10). This implies that overexpression of bHLH061 can influence root development. The variation in the root length among the bHLH061ox root measurements was substantial, ranging from 9 mm to 37 mm. This is in contrast to WT, which ranged from 10 mm to 22 mm. It was unclear what caused the wide variation within a single genotype, but larger plates could be used in future iterations of this experiment to allow for additional spacing of seedlings and limit the possibility that interactions between neighboring roots resulting in inconsistent growth not related to genotype.

Flowering time

bHLH061 ox and bHLH093 ox a change in flowering habit compared to WT. Although no consistent difference in leaf shape was observed, bHLH061 ox and bHLH093 ox plants produced significantly more leaves prior to flowering compared to WT (19.4 vs

11.8 leaves p = 3 x 10^{-5} for bHLH061 ox and 23.0 vs 11.8 leaves for bHLH093 ox

p = 3.9 x 10^{-7}) (Figure 10). Determination of leaf number prior to flowering is a common

assay for determining delays in flowering time in Arabidopsis (Koornneef et al., 1991).

Consistent with the increase in leaf number, both bHLH061 ox and bHLH093 ox had a

significant increase in days to flowering (49 and 48 days, respectively, compared to 34 days

for WT, p = 5 x 10^{-9}) (Figure 11).

In addition to an increase in leaf number and days to flowering, both bHLH061 ox

and bHLH093 ox exhibited more than one inflorescence at initial flowering contributing to

a bushy phenotype compared to WT (Figure 12). In Arabidopsis, inflorescence

development generally occurs via a single central inflorescence with additional

inflorescences produced over time based on apical dominance of the primary central

inflorescence. bHLH061 ox and bHLH093 ox plants had an average of two initial

inflorescences emerge at first flowering (Figure 12 and Figure 13, Table 11), which is an

unusual growth habit for Arabidopsis and indicates a clear loss of apical dominance in

overexpressing lines.

In summary, all of the flowering parameters investigated (number of rosette leaves

at flowering, time in days of flowering, and number of concurrent inflorescences at

flowering) display a significant phenotypic difference between bHLH061 ox or bHLH093

ox, and WT.

Stomata production

To analyze changes in stomatal development, I observed the abaxial surface of true

leaves using light microscopy (Figure 1). The abaxial surfaces of true leaves of bHLH061 ox

and bHLH093 ox plants were analyzed for changes in stomatal patterning and development (Figure 14). I didn't observe any obvious anomalies in the number, appearance, or density of the stomata in bHLH061 ox and bHLH093 ox compared to WT. Stomatal index (SI) (Salisbury, 1928) is the ratio of the number of epidermal cells to the number of stomata in a given leaf area. SI is commonly used instead of total number of stomata to normalize stomata number to the amount of cell divisions taking place. Overexpression of bHLH061 produced a small, but significant decrease in SI compared to WT (0.16 vs 0.18; p=0.02) but bHLH093 ox SI did not differ from WT (Figure 15). I also determined the average number of stomatal doubles (two adjacent stomata) for each plant line. The number of doubles observed/leaf was close to zero for all genotypes (Figure 16).

Characterization of bHLH061 and bHLH093 transcriptional knockout lines.

In addition to evaluating the phenotypes of plants ectopically overexpressing bHLH061 and bHLH093, I analyzed their loss-of-function phenotypes using publicly available T-DNA insertion lines. The insertion lines used for evaluation were CS844212 for At5g10570 (*bhlh061*) (Figure 17a) and SALK_121082 for At5g65640 (*bhlh093*) (Figure 17b). The location of the insertions for both *bhlh093* and *bhlh063* was predicted to be highly detrimental to gene expression due to the disruption of the ORF of each gene. The *bHLH061* T-DNA insertion is located within the second intron, whereas the *bHLH093* T-DNA insertion is located in the first exon (Figure 17). To confirm the presence of the T-DNA insert in each mutant line, I performed PCR using primers specific to either *bHLH061* or *bHLH093* and a T-DNA left-border primer. Plants segregating for the T-DNA insertion were analyzed for the homozygous presence of the T-DNA insertion. Based on these results, I

identified homozygous mutants, *bhlh061* and *bhlh093,* to use for further analysis and genetic crosses (Figure 18). To identify any functional redundancy between bHLH061 and bHLH093, I produced a double loss-of-function mutant (*bhlh093xbhlh061*) through directed outcrossing between homozygous mutant *bhlh061* and *bhlh093* plants and genotyped F1 offspring to confirm the presence of the T-DNA inserts. The F1 generation was allowed to self-fertilize, and homozygous double mutant plants were confirmed using PCR in the F3 population.

Confirmation of loss of detectable transcript in single and double mutants

Although the annotated insertion location for both *bHLH061* and *bHLH093* are predicted to be detrimental (both inserts are early in the coding sequence), I confirmed that the inserts resulted in loss of detectable transcript. I performed RT-PCR on single and double mutant lines, *bhlh093*, *bhlh061,* and *bhlh093xbhlh061*, to determine that all were transcriptional knockout lines. No bHLH093 transcripts could be detected in SALK_121082, which is consistent with the results from Sharma et al., 2016 who detected no transcripts in this insertion line. I determined that insertion line CS844212 produced no detectable *bHLH061* transcripts. Consistently, no transcripts of *bHLH061* and *bHLH093* were identified in the double mutant (Figure 19).

Loss of bHLH061 and bHLH093 has minimal impact on phenotype.

Plant Height

Plant height was measured at the start of senescence for *bhlh061*, *bhlh093,* and *bhlh093xbhlh061* and compared to WT (Figure 20). The final heights of *bhlh061*, *bhlh093,* and *bhlh093xbhlh061* plants did not differ phenotypically from WT.

Root length

Root length for *bhlh061*, *bhlh093,* and *bhlh093xbhlh061* was averaged for all genotypes. In both single and double mutant lines, the average root length was not different from WT (Figure 21). However, of the averaged root lengths, *bhlh061* plants tended to have a shorter average root length (20.9mm) compared to *bhlh093* (24.2mm), *bhlh093xbhlh061* (25.4mm) or WT (25.7mm) plants. Similar to the results of the overexpressing lines, there was a wide variation in the *bhlh061* root lengths from 6mm to 40mm. The trend toward shorter average root length for *bhlh061* contrasts the results of overexpression, where bHLH061 ox plants had roots that were significantly longer than WT. As suggested for overexpressing plants, further investigation of root length with larger plates might allow discrimination between a potential effect of the genotype and experimental conditions.

Flowering time

To investigate the role of these genes on flowering time, I analyzed the leaf number at inflorescence emergence. The number of leaves of *bhlh061* and the *bhlh093xbhlh061* cross were not different from WT. However, the *bhlh093* plants showed a small increase in

leaf number compared to the WT (14.4 vs 11.8, p = 0.02). Because of our stringent

Bonferroni correction, this increase in leaf number is not significant, but it shows a clear

trend toward more leaves, which is supported by the number of days to flowering for

bhlh093.

In addition this analysis would benefit from larger samples sizes, days to flowering

data was consistent with leaf number as expected. Compared to WT, neither *bhlh061* nor

bhlh093xbhlh061 had a difference in days to flowering. The *bhlh093* plants, however,

trended toward more days to flowering compared to WT (Figure 23). Again, based on our

stringent correction, this trend was not significant (p = 0.02). We feel a larger samples size

is required to establish a robust conclusion from these data. It isn't clear why the loss of

bHLH093 produces noticeable phenotypic changes, but those changes are not also seen in

the double mutant.

In addition to flowering time, I analyzed the average number of inflorescences

produced at flowering. bHLH061 ox and bHLH093 ox plants had a clear impact on

inflorescence production, producing an average of two inflorescences at flowering implying

that apical dominance was inhibited or interrupted. In contrast, *bhlh061*, *bhlh093*, and

bhlh093xbhlh061 conformed to the Arabidopsis standard growth habit of a single

inflorescence at flowering (Figure 24).

Stomata production

I predicted that the loss-of-function of *bHLH093* may disrupt stomatal development.

Based on this study, there were no obvious anomalies to the appearance of stomata or

number of stomata in *bhlh093*, *bhlh061*, or *bhlh093xbhlh061* (Figure 25). All stomata were

composed of two guard cells with no visually detectable defects. I also investigated the SI and presence of clustered stomata on the abaxial surface. SI for all mutant plant lines was not different from WT (Figure 26).

The number of stomatal doubles (Figure 27) identified in mutant lines was variable and very low (1-2 doubles/leaf) (Figure 28). However, doubles were almost never identified on WT leaves in this experiment and it has been shown consistently in the literature over the last decade that doubles are rarely seen in WT plants (Bergmann et al., 2004; Ohashi-Ito and Bergmann, 2006; Pillitteri et al., 2007). Stomatal doubles (Figure 27) are very rare in WT plants because stomata are generated by a complex developmental program that ensures stomata are placed at least one cell apart from one another, the so called "one-cell-spacing" rule (Nadeau and Sack, 2002). The low number identified makes it difficult to make a strong conclusion. However, the fact that doubles are present at all is noteworthy. This parameter could be looked at in the future in combination with stomatal spacing mutants, such as TOO MANY MOUTHS (TMM) (Nadeau and Sack, 2002) or under SD/high intensity light conditions to better address a role in stomatal development.

Discussion

While the potential role of bHLH061 and bHLH093 in stomatal development was the initial motivator for this study, there was no knowledge of their function when this work was initiated. Here, I investigated the phenotypic impact of ectopic overexpression and loss-of-function of both genes to improve our understanding of their role in development. Overall, I determined that ectopic overexpression of either bHLH061 or bHLH093 produced several phenotypic changes in growth, whereas more minimal changes were observed in loss-of-function mutants under the conditions used in this study. It is important to note that two articles have been published that establish that bHLH093 and bHLH061 have a role in flowering and meristem function and that their function is strongly impacted by both high-light intensity and SD photoperiod. Because my study was carried out under LD photoperiod and low-medium light intensity, my data provides additional information to gain insight about these two transcriptional regulators.

Poirier et al. (Poirier et al., 2018) did not investigate bHLH061 overexpression, but did conclude that bHLH093 ectopic overexpression did not alter final plant height under high light intensity conditions. I produced transgenic plants that ectopically express either bHLH061 or bHLH093 and determined that final plant height was not different from WT under low to medium-light conditions. Therefore, our results are in agreement with published results, even under different conditions, and imply that bHLH093 and bHLH061 are not involved in height determination in Arabidopsis. This was supported by the fact that single and double mutants, *bhlh093, bhlh061,* and *bhlh093xbhlh061*, also displayed no change in final height compared to WT (Figure 20). Because published results have

established these transcription factors function in the translation of specific light cues to promote the transition to reproductive growth (flowering), it is perhaps not surprising that height (post floral transition trait) is not affected.

Contrary to height, my results suggest that ectopic overexpression of either bHLH061 or bHLH093 cause a delay in flowering (Koornneef et al., 1991). bHLH061 ox and bHLH093 ox both flowered later than WT and had an associated increase in the number of rosette leaves at flowering compared to WT. This indicates that overexpression or ectopic expression interferes with normal meristem transition from vegetative to reproductive growth even under the LD conditions used in this study. Both overexpressing lines also produced more concurrent inflorescences compared to WT, which indicates a loss of apical dominance in the primary meristem. Taken together, these data strongly suggests that our overexpression lines interrupt internal and external signaling networks in the apical meristem that promote flowering. Interestingly, Poirier et al. did not observe these flowering abnormalities in their study of bHLH093 overexpression under high light intensity. However, both Sharma et al. and Poirier et al. did observe similar, but more severe versions of these defects when investigating transcriptional loss-of-function mutants under SD and high-light intensity conditions, respectively. Published results indicate that loss of bHLH093 or bHLH061 does not result in a change in flowering or any phenotypic character under LD conditions. In contrast to those results, our data did indicate a small delay in flowering time in the *bhlh093* mutant compared to WT. While my results show that only *bhlh093* had a trend toward a delay in flowering time, it bears mentioning that the difference in number of leaves (14.1 and 14.4 leaves on average,

compared to 11.8 for WT) and days to flowering (38.4 and 38.2 days vs 34.8 days for WT) for *bhlh093* and *bhlh061* was minimal.

Taken together, we cannot rule out that these genes play a modest role in flowering time under LD, but acknowledge that they have a critical and required role in flowering under SD when promotive light cues are not present. Larger sampling could help determine a true effect on these flowering parameters in the single and double mutants under LD. Because the function of these genes is tightly linked to light, it is possible that even transient changes in light intensity (moving plants from growth room to lab) could impact phenotypes related to the single and double mutants. These would need to be carefully considered in future experiments.

Root length was not investigated by either Sharma et al. (Sharma et al., 2016) or Poirier et al. (Poirier et al., 2018). Sharma et al. did observe the expression of bHLH093 in root tips under both SD and LD conditions, suggesting it may have a function in root meristem in addition to the apical meristem. Neither paper analyzed the expression of bHLH061 in the root tip, so it is not known if it is endogenously expressed there.

I found a robust significant increase in root length in bHLH061 ox and a trend toward an average decrease in root length in *bhlh061* compared to WT, which suggests that bHLH061 may play a promotive role in root growth. Poirier et al. hypothesize that all members of subgroup IIIb (Heim et al., 2003) are involved in regulating and/or determining the function of meristematic cells in Arabidopsis. It is possible that bHLH061 overexpression in the root tip under control of the CaMV constitutive promoter influenced root length by acting on the root apical meristem (Dolan et al., 1993) through endogenous or non-endogenous binding partners. Our observations of multiple transcript bands in our

43

overexpression lines (Figure 6) could also impact endogenous interactions in unpredictable ways. Further investigation of the localization and expression of bHLH061, root structural analysis and combination mutant analysis with root development genes such as SHORT ROOT (SHR) or SCRARECROW (SCR) (Helariutta et al., 2000; Laurenzio et al., 1996) could provide evidence to support or refute a role of bHLH061 at the root apical meristem.

Overall, we identified several phenotypic changes related to alterations in bHLH093 and bHLH061 gene expression, but we started this study because several lines of evidence supported a potential role for bHLH093 in the stomatal development pathway (Ohashi-Ito and Bergmann, 2006) (Pillitteri, unpublished). On direct observation, stomata shape and density did not look different from WT across any of the genotypes used in this study. Upon more careful counting, the stomatal index was slightly lower for bHLH061 ox compared to bHLH093 ox and WT. Interestingly, the transcriptional loss-of-function of either bHLH061 or bHLH093 did not produce a change in stomatal index compared to WT. However, the number of double stomata appeared to increase modestly in *bhlh093xbhlh061* compared to WT.

If this increase in stomatal doubles is confirmed through higher sampling, it may indicate that that bHLH061 and bHLH093 can redundantly impact stomatal developmental. However, it would be unlikely to be based on an interaction with either FAMA or MUTE because neither *mute* or *fama* mutants produce an increase in adjacent stomata (Ohashi-Ito and Bergmann, 2006; Pillitteri et al., 2007). Overall, we identified no phenotypic evidence that would imply that either bHLH093 or bHLH061 bind with FAMA or MUTE endogenously. An alternate role in stomata development could be investigated related to

gibberellin biosynthesis or signaling if higher sampling confirms these initial results of an increase in stomatal doubles.

The different growth conditions (LD and low-medium light intensity versus SD and high-light intensity) used in these studies do not allow for direct comparison of our data with that of Sharma et al. (Sharma et al., 2016) and Poirier et al. (Poirier et al., 2018). However, the data presented here and those in published studies observe a disruption of flowering and loss of apical dominance when bHLH061 or bHLH093 expression is perturbed. Sharma et al. (Sharma et al., 2016) named bHLH093 NFL (NO FLOWERING IN SHORT DAY) and discussed its role in flowering under SD conditions, whereas, Poirier et al. (Poirier et al., 2018) described its involvement in general meristem maintenance under high-light intensity conditions. Together, these studies established that bHLH061 and bHLH093 play a role in maintaining the identity of the shoot apical meristem (SAM) and are required for flowering under SD and high light intensity conditions.

Apical dominance and meristem maintenance are regulated by complex interactions between phytohormones and transcription factors that are beyond the scope of this study (Hayward et al., 2009; Müller et al., 2015; Shani et al., 2006; Snow, 1937). I determined that *bhlh061*, *bhlh093*, and *bhlh093xbhlh061* all had one inflorescence emerge at flowering, clearly indicating that apical dominance was not impacted under LD. This would be consistent with that the idea that these genes play a minimal role in development under LD conditions when multiple other pathways converge to regulate meristem function and flowering time to ensure reproductive success.

Poirier et al. found that the depletion of endogenous gibberellin in loss-of-function mutants led to the deterioration of the SAM and loss of apical dominance. Based on our

results, the constitutive overexpression of bHLH061 and bHLH093 at the transcriptional level could have resulted in a suppression of these genes post-transcriptionally as has been documented many times in plant literature (Eamens et al., 2008; van der Krol et al., 1990; Napoli et al., 1990). The suppression of bHLH093 and bHLH061 expression could impact gibberellin production, mimicking the loss-of-function phenotypes observed in the other studies. This scenario is unlikely based on the fact that loss-of-function mutants under LD in this study did not have significant flowering defects as was observed for bHLH093 ox and bHLH062 ox. This implies that our overexpression plants are not simply repressing bHLH093 and bHLH061 expression, although we cannot exclude that possibility. Close examination of the meristem would provide structural evidence to support an alternate hypothesis that higher levels of gibberellin production due to ectopic overexpression or non-endogenous interactions of bHLH093 and bHLH061 with other binding partners could also interrupt flowering and apical dominance in unforeseen or unpredictable ways.

Literature Cited

Abreu, R. de S., Penalva, L.O., Marcotte, E.M., and Vogel, C. (2009). Global signatures of protein and mRNA expression levels. Mol. Biosyst. *5*, 1512–1526.

Ache, P., Bauer, H., Kollist, H., Al-Rasheid, K.A.S., Lautner, S., Hartung, W., and Hedrich, R. (2010). Stomatal action directly feeds back on leaf turgor: new insights into the regulation of the plant water status from non-invasive pressure probe measurements. Plant J. *62*, 1072–1082.

Amack, S.C., and Antunes, M.S. (2020). CaMV35S promoter – A plant biology and biotechnology workhorse in the era of synthetic biology. Curr. Plant Biol. *24*, 100179.

Atchley, W.R., and Fitch, W.M. (1997). A natural classification of the basic helix–loop–helix class of transcription factors. Proc. Natl. Acad. Sci. *94*, 5172–5176.

Balcerowicz, M., and Hoecker, U. (2014). Auxin – a novel regulator of stomata differentiation. Trends Plant Sci. *19*, 747–749.

Belfield, E.J., Ding, Z.J., Jamieson, F.J.C., Visscher, A.M., Zheng, S.J., Mithani, A., and Harberd, N.P. (2018). DNA mismatch repair preferentially protects genes from mutation. Genome Res. *28*, 66–74.

Benfey, P.N., and Chua, N.-H. (1990). The Cauliflower Mosaic Virus 35S Promoter: Combinatorial Regulation of Transcription in Plants. Science *250*, 959–966.

Bergmann, D.C., Lukowitz, W., and Somerville, C.R. (2004). Stomatal Development and Pattern Controlled by a MAPKK Kinase. Science *304*, 1494–1497.

Boyes, D.C., Zayed, A.M., Ascenzi, R., McCaskill, A.J., Hoffman, N.E., Davis, K.R., and Görlach, J. (2001). Growth Stage –Based Phenotypic Analysis of Arabidopsis. Plant Cell *13*, 1499–1510.

Bruex, A., Kainkaryam, R.M., Wieckowski, Y., Kang, Y.H., Bernhardt, C., Xia, Y., Zheng, X., Wang, J.Y., Lee, M.M., Benfey, P., et al. (2012). A Gene Regulatory Network for Root Epidermis Cell Differentiation in Arabidopsis. PLoS Genet. *8*, e1002446.
Cantín, C.M., Fidelibus, M.W., and Crisosto, C.H. (2007). Application of abscisic acid (ABA) at veraison advanced red color development and maintained postharvest quality of 'Crimson Seedless' grapes. Postharvest Biol. Technol. *46*, 237–241.

Chater, C.C.C., Caine, R.S., Fleming, A.J., and Gray, J.E. (2017). Origins and Evolution of Stomatal Development. Plant Physiol. *174*, 624–638.

Chen, X., Huang, H., Qi, T., Liu, B., and Song, S. (2016). New perspective of the bHLH-MYB complex in jasmonate-regulated plant fertility in arabidopsis. Plant Signal. Behav. *11*, e1135280.

Cheng, Y., and Perocchi, F. (2015). ProtPhylo: identification of protein–phenotype and protein–protein functional associations via phylogenetic profiling. Nucleic Acids Res. *43*, W160–W168.

Chinnusamy, V., Ohta, M., Kanrar, S., Lee, B., Hong, X., Agarwal, M., and Zhu, J.-K. (2003). ICE1: a regulator of cold-induced transcriptome and freezing tolerance in Arabidopsis. Genes Dev. *17*, 1043–1054.

Clough, S.J., and Bent, A.F. (1998). Floral dip: a simplified method for Agrobacterium - mediated transformation of Arabidopsis thaliana. Plant J. *16*, 735–743.

Dey, G., Jaimovich, A., Collins, S.R., Seki, A., and Meyer, T. (2015). Systematic Discovery of Human Gene Function and Principles of Modular Organization through Phylogenetic Profiling. Cell Rep. *10*, 993–1006.

Dinneny, J.R., and Benfey, P.N. (2008). Plant Stem Cell Niches: Standing the Test of Time. Cell *132*, 553–557.

Dolan, L., Janmaat, K., Willemsen, V., Linstead, P., Poethig, S., Roberts, K., and Scheres, B. (1993). Cellular organisation of the Arabidopsis thaliana root. Dev. Camb. Engl. *119*, 71–84.

Eamens, A., Wang, M.-B., Smith, N.A., and Waterhouse, P.M. (2008). RNA Silencing in Plants: Yesterday, Today, and Tomorrow. Plant Physiol. *147*, 456–468.

Edwards, D., Kerp, H., and Hass, H. (1998). Stomata in early land plants: an anatomical and ecophysiological approach. J. Exp. Bot. *49*, 255–278.

Elhaddad, N.S., Hunt, L., Sloan, J., and Gray, J.E. (2014). Light-Induced Stomatal Opening Is Affected by the Guard Cell Protein Kinase APK1b. PLoS ONE *9*.

Franks, P.J., W. Doheny-Adams, T., Britton-Harper, Z.J., and Gray, J.E. (2015). Increasing water-use efficiency directly through genetic manipulation of stomatal density. New Phytol. *207*, 188–195.

Furner, I.J. (1992). THE VERTICAL-PLATE ASSAY FOR DRUG RESISTANCE IN ARABIDOPSIS. Www.Arabidopsis.Org.

Gordân, R., Shen, N., Dror, I., Zhou, T., Horton, J., Rohs, R., and Bulyk, M.L. (2013). Genomic regions flanking E-box binding sites influence DNA binding specificity of bHLH transcription factors through DNA shape. Cell Rep. *3*, 1093–1104.

Groß-Hardt, R., and Laux, T. (2003). Stem cell regulation in the shoot meristem. J. Cell Sci. *116*, 1659–1666.

Han, X., Hu, Y., Zhang, G., Jiang, Y., Chen, X., and Yu, D. (2018). Jasmonate Negatively Regulates Stomatal Development in Arabidopsis Cotyledons1. Plant Physiol. *176*, 2871–2885.

Hao, Y., Oh, E., Choi, G., Liang, Z., and Wang, Z.-Y. (2012). Interactions between HLH and bHLH Factors Modulate Light-Regulated Plant Development. Mol. Plant *5*, 688–697.

Hao, Y., Zong, X., Ren, P., Qian, Y., and Fu, A. (2021). Basic Helix-Loop-Helix (bHLH) Transcription Factors Regulate a Wide Range of Functions in Arabidopsis. Int. J. Mol. Sci. *22*, 7152.

Hara, K., Kajita, R., Torii, K.U., Bergmann, D.C., and Kakimoto, T. (2007). The secretory peptide gene EPF1 enforces the stomatal one-cell-spacing rule. Genes Dev. *21*, 1720–1725.

Hayward, A., Stirnberg, P., Beveridge, C., and Leyser, O. (2009). Interactions between Auxin and Strigolactone in Shoot Branching Control. Plant Physiol. *151*, 400–412.

Heim, M.A., Jakoby, M., Werber, M., Martin, C., Weisshaar, B., and Bailey, P.C. (2003). The Basic Helix–Loop–Helix Transcription Factor Family in Plants: A Genome-Wide Study of Protein Structure and Functional Diversity. Mol. Biol. Evol. *20*, 735–747.

Helariutta, Y., Fukaki, H., Wysocka-Diller, J., Nakajima, K., Jung, J., Sena, G., Hauser, M.-T., and Benfey, P.N. (2000). The SHORT-ROOT Gene Controls Radial Patterning of the Arabidopsis Root through Radial Signaling. Cell *101*, 555–567.

Ishizaki, K. (2017). Evolution of land plants: insights from molecular studies on basal lineages. Biosci. Biotechnol. Biochem. *81*, 73–80.

Jiang, W., Zhou, H., Bi, H., Fromm, M., Yang, B., and Weeks, D.P. (2013). Demonstration of CRISPR/Cas9/sgRNA-mediated targeted gene modification in Arabidopsis, tobacco, sorghum and rice. Nucleic Acids Res. *41*, e188.

Jones, S. (2004). An overview of the basic helix-loop-helix proteins. Genome Biol. *5*, 226–226.

Kanaoka, M.M., Pillitteri, L.J., Fujii, H., Yoshida, Y., Bogenschutz, N.L., Takabayashi, J., Zhu, J.-K., and Torii, K.U. (2008). SCREAM/ICE1 and SCREAM2 Specify Three Cell-State Transitional Steps Leading to Arabidopsis Stomatal Differentiation. Plant Cell *20*, 1775–1785.

Koornneef, M., Hanhart, C.J., and van der Veen, J.H. (1991). A genetic and physiological analysis of late flowering mutants in Arabidopsis thaliana. Mol. Gen. Genet. MGG *229*, 57–66.

Kostaki, K.-I., Coupel-Ledru, A., Bonnell, V.C., Gustavsson, M., Sun, P., Mclaughlin, F.J., Fraser, D.P., McLachlan, D.H., Hetherington, A.M., Dodd, A.N., et al. (2020). Guard cells integrate light and temperature signals to control stomatal aperture. Plant Physiol.

van der Krol, A.R., Mur, L.A., Beld, M., Mol, J.N., and Stuitje, A.R. (1990). Flavonoid genes in petunia: addition of a limited number of gene copies may lead to a suppression of gene expression. Plant Cell *2*, 291–299.

Lai, L.B., Nadeau, J.A., Lucas, J., Lee, E.-K., Nakagawa, T., Zhao, L., Geisler, M., and Sack, F.D. (2005). The Arabidopsis R2R3 MYB Proteins FOUR LIPS and MYB88 Restrict Divisions Late in the Stomatal Cell Lineage. Plant Cell *17*, 2754–2767.

Lampard, G.R., Macalister, C.A., and Bergmann, D.C. (2008). Arabidopsis stomatal initiation is controlled by MAPK-mediated regulation of the bHLH SPEECHLESS. Science *322*, 1113–1116.

Larkin, J.C., Marks, M.D., Nadeau, J., and Sack, F. (1997). Epidermal cell fate and patterning in leaves. Plant Cell *9*, 1109–1120.

Lau, O.S., and Bergmann, D.C. (2012). Stomatal development: a plant's perspective on cell polarity, cell fate transitions and intercellular communication. Dev. Camb. Engl. *139*, 3683–3692.

Lau, O.S., Davies, K.A., Chang, J., Adrian, J., Rowe, M.H., Ballenger, C.E., and Bergmann, D.C. (2014). Direct roles of SPEECHLESS in the specification of stomatal self-renewing cells. Science *345*, 1605–1609.

Laurenzio, L.D., Wysocka-Diller, J., Malamy, J.E., Pysh, L., Helariutta, Y., Freshour, G., Hahn, M.G., Feldmann, K.A., and Benfey, P.N. (1996). The SCARECROW Gene Regulates an Asymmetric Cell Division That Is Essential for Generating the Radial Organization of the Arabidopsis Root. Cell *86*, 423–433.

Ledent, V., Paquet, O., and Vervoort, M. (2002). Phylogenetic analysis of the human basic helix-loop-helix proteins. Genome Biol. *3*, RESEARCH0030–RESEARCH0030.

Lee, S.B., Kim, H., Kim, R.J., and Suh, M.C. (2014). Overexpression of Arabidopsis MYB96 confers drought resistance in Camelina sativa via cuticular wax accumulation. Plant Cell Rep. *33*, 1535–1546.

Liu, T., Ohashi-Ito, K., and Bergmann, D.C. (2009). Orthologs of Arabidopsis thaliana stomatal bHLH genes and regulation of stomatal development in grasses. Dev. Camb. Engl. *136*, 2265–2276.

Luo, J., Butelli, E., Hill, L., Parr, A., Niggeweg, R., Bailey, P., Weisshaar, B., and Martin, C. (2008). AtMYB12 regulates caffeoyl quinic acid and flavonol synthesis in tomato: expression in fruit results in very high levels of both types of polyphenol. Plant J. Cell Mol. Biol. *56*, 316–326.

MacAlister, C.A., and Bergmann, D.C. (2011). Sequence and function of basic helix-loop-helix proteins required for stomatal development in Arabidopsis are deeply conserved in land plants. Evol. Dev. *13*, 182–192.

MacAlister, C.A., Ohashi-Ito, K., and Bergmann, D.C. (2007). Transcription factor control of asymmetric cell divisions that establish the stomatal lineage. Nature *445*, 537–540.

Massari, M., and Murre, C. (2000). Helix-Loop-Helix Proteins: Regulators of Transcription in Eucaryotic Organisms. Mol. Cell. Biol. *20*, 429–440.

Mayer, K.F.X., Schoof, H., Haecker, A., Lenhard, M., Jürgens, G., and Laux, T. (1998). Role of WUSCHEL in Regulating Stem Cell Fate in the Arabidopsis Shoot Meristem. Cell *95*, 805–815.

Meinke, D.W., Cherry, J.M., Dean, C., Rounsley, S.D., and Koornneef, M. (1998). Arabidopsis thaliana: A Model Plant for Genome Analysis. Science *282*, 662.

Melotto, M., Underwood, W., Koczan, J., Nomura, K., and He, S.Y. (2006). Plant Stomata Function in Innate Immunity against Bacterial Invasion. Cell *126*, 969–980.

Mitre, L.K., Teixeira-Silva, N.S., Rybak, K., Magalhães, D.M., Souza-Neto, R.R. de, Robatzek, S., Zipfel, C., and Souza, A.A. de (2021). The Arabidopsis immune receptor EFR increases resistance to the bacterial pathogens Xanthomonas and Xylella in transgenic sweet orange. Plant Biotechnol. J. *19*, 1294–1296.

Mitsuda, N., and Ohme-Takagi, M. (2009). Functional analysis of transcription factors in Arabidopsis. Plant Cell Physiol. *50*, 1232–1248.

Müller, D., Waldie, T., Miyawaki, K., To, J.P.C., Melnyk, C.W., Kieber, J.J., Kakimoto, T., and Leyser, O. (2015). Cytokinin is required for escape but not release from auxin mediated apical dominance. Plant J. *82*, 874–886.

Murre, C., McCaw, P.S., Vaessin, H., Caudy, M., Jan, L.Y., Jan, Y.N., Cabrera, C.V., Buskin, J.N., Hauschka, S.D., Lassar, A.B., et al. (1989). Interactions between heterologous helix-loop-helix proteins generate complexes that bind specifically to a common DNA sequence. Cell *58*, 537–544.

Nadeau, J.A., and Sack, F.D. (2002). Control of stomatal distribution on the Arabidopsis leaf surface. Science *296*, 1697–1700.

Nakagawa, T., Kurose, T., Hino, T., Tanaka, K., Kawamukai, M., Niwa, Y., Toyooka, K., Matsuoka, K., Jinbo, T., and Kimura, T. (2007). Development of series of gateway binary vectors, pGWBs, for realizing efficient construction of fusion genes for plant transformation. J. Biosci. Bioeng. *104*, 34–41.

Napoli, C., Lemieux, C., and Jorgensen, R. (1990). Introduction of a Chimeric Chalcone Synthase Gene into Petunia Results in Reversible Co-Suppression of Homologous Genes in trans. Plant Cell *2*, 279–289.

Ohashi-Ito, K., and Bergmann, D.C. (2006). Arabidopsis FAMA Controls the Final Proliferation/Differentiation Switch during Stomatal Development. Plant Cell *18*, 2493–2505.

Ortega, A., de Marcos, A., Illescas-Miranda, J., Mena, M., and Fenoll, C. (2019). The Tomato Genome Encodes SPCH, MUTE, and FAMA Candidates That Can Replace the Endogenous Functions of Their Arabidopsis Orthologs. Front. Plant Sci. *10*.

Perez-Vizcaino, F., and Duarte, J. (2010). Flavonols and cardiovascular disease. Mol. Aspects Med. *31*, 478–494.

Peterson, K.M., Rychel, A.L., and Torii, K.U. (2010). Out of the Mouths of Plants: The Molecular Basis of the Evolution and Diversity of Stomatal Development. Plant Cell *22*, 296.

Pillitteri, L.J., Sloan, D.B., Bogenschutz, N.L., and Torii, K.U. (2007). Termination of asymmetric cell division and differentiation of stomata. Nature *445*, 501–505.

Pillitteri, L.J., Peterson, K.M., Horst, R.J., and Torii, K.U. (2011). Molecular Profiling of Stomatal Meristemoids Reveals New Component of Asymmetric Cell Division and Commonalities among Stem Cell Populations in Arabidopsis. Plant Cell *23*, 3260–3275.

Plotkin, J.B. (2010). Transcriptional regulation is only half the story. Mol. Syst. Biol. *6*, 406.

Poirier, B.C., Feldman, M.J., and Lange, B.M. (2018). bHLH093/NFL and bHLH061 are required for apical meristem function in Arabidopsis thaliana. Plant Signal. Behav. *13*, e1486146.

Putarjunan, A., Ruble, J., Srivastava, A., Zhao, C., Rychel, A.L., Hofstetter, A.K., Tang, X., Zhu, J.-K., Tama, F., Zheng, N., et al. (2019). Bipartite anchoring of SCREAM enforces stomatal initiation by coupling MAP Kinases to SPEECHLESS. Nat. Plants *5*, 742–754.

Ran, J.-H., Shen, T.-T., Liu, W.-J., and Wang, X.-Q. (2013). Evolution of the bHLH genes involved in stomatal development: implications for the expansion of developmental complexity of stomata in land plants. PloS One *8*, e78997.

Richardson, L.G.L., and Torii, K.U. (2013). Take a deep breath: peptide signalling in stomatal patterning and differentiation. J. Exp. Bot. *64*, 5243–5251.

Riechmann, J.L., Heard, J., Martin, G., Reuber, L., Jiang, C., Keddie, J., Adam, L., Pineda, O., Ratcliffe, O.J., Samaha, R.R., et al. (2000). Arabidopsis transcription factors: genome-wide comparative analysis among eukaryotes. Science *290*, 2105–2110.

Salisbury, E.J. (1928). On the Causes and Ecological Significance of Stomatal Frequency, with Special Reference to the Woodland Flora. Philos. Trans. R. Soc. Lond. Ser. B Contain. Pap. Biol. Character *216*, 1–65.

Schlüter, U., Muschak, M., Berger, D., and Altmann, T. (2003). Photosynthetic performance of an Arabidopsis mutant with elevated stomatal density (sdd1-1) under different light regimes. J. Exp. Bot. *54*, 867–874.

Scofield, S., and Murray, J.A.H. (2006). The Evolving Concept of the Meristem. Plant Mol. Biol. *60*, V–VII.

Shani, E., Yanai, O., and Ori, N. (2006). The role of hormones in shoot apical meristem function. Curr. Opin. Plant Biol. *9*, 484–489.

Sharma, N., Xin, R., Kim, D.-H., Sung, S., Lange, T., and Huq, E. (2016). NO FLOWERING IN SHORT DAY (NFL) is a bHLH transcription factor that promotes flowering specifically under short-day conditions in Arabidopsis. Development *143*, 682–690.

Shpak, E.D., McAbee, J.M., Pillitteri, L.J., and Torii, K.U. (2005). Stomatal Patterning and Differentiation by Synergistic Interactions of Receptor Kinases. Science *309*, 290–293.

Snow, R. (1937). On the Nature of Correlative Inhibition. New Phytol. *36*, 283–300.

Splettstoesser, T. (2007). Basic-helix-loop-helix structural motif of proteins. Two helices (blue) are connected by a short loop region (red). Based on the structure of Aryl hydrocarbon receptor nuclear translocator (ARNT): PDB ID 1X0o.

Sugano, S.S., Shimada, T., Imai, Y., Okawa, K., Tamai, A., Mori, M., and Hara-Nishimura, I. (2010). Stomagen positively regulates stomatal density in Arabidopsis. Nature *463*, 241–244.

Tamnanloo, F., Damen, H., Jangra, R., and Lee, J.S. (2018). MAP KINASE PHOSPHATASE1 Controls Cell Fate Transition during Stomatal Development. Plant Physiol. *178*, 247–257.

Tanaka, Y., Sugano, S.S., Shimada, T., and Hara-Nishimura, I. (2013). Enhancement of leaf photosynthetic capacity through increased stomatal density in Arabidopsis. New Phytol. *198*, 757–764.

The Arabidopsis Genome Initiative (2000). Analysis of the genome sequence of the flowering plant Arabidopsis thaliana. Nature *408*, 796–815.

Toledo-Ortiz, G., Huq, E., and Quail, P.H. (2003). The Arabidopsis Basic/Helix-Loop-Helix Transcription Factor Family. Plant Cell *15*, 1749–1770.

Van Daele, I., Gonzalez, N., Vercauteren, I., de Smet, L., Inzé, D., Roldán-Ruiz, I., and Vuylsteke, M. (2012). A comparative study of seed yield parameters in Arabidopsis thaliana mutants and transgenics. Plant Biotechnol. J. *10*, 488–500.

Vogel, C., and Marcotte, E.M. (2012). Insights into the regulation of protein abundance from proteomic and transcriptomic analyses. Nat. Rev. Genet. *13*, 227–232.

Wengier, D.L., and Bergmann, D.C. (2012). On fate and flexibility in stomatal development. Cold Spring Harb. Symp. Quant. Biol. *77*, 53–62.

Wilson, R.N., Heckman, J.W., and Somerville, C.R. (1992). Gibberellin Is Required for Flowering in Arabidopsis thaliana under Short Days. Plant Physiol. *100*, 403–408.

Wood, V., Lock, A., Harris, M.A., Rutherford, K., Bähler, J., and Oliver, S.G. Hidden in plain sight: what remains to be discovered in the eukaryotic proteome? Open Biol. *9*, 180241.

Wu, Z., Chen, L., Yu, Q., Zhou, W., Gou, X., Li, J., and Hou, S. (2019). Multiple transcriptional factors control stomata development in rice. New Phytol. *223*, 220–232.

Yoo, C.Y., Hasegawa, P.M., and Mickelbart, M.V. (2011). Regulation of stomatal density by the GTL1 transcription factor for improving water use efficiency. Plant Signal. Behav. *6*, 1069–1071.

Yu, H., Ito, T., Zhao, Y., Peng, J., Kumar, P., and Meyerowitz, E.M. (2004). Floral homeotic genes are targets of gibberellin signaling in flower development. Proc. Natl. Acad. Sci. U. S. A. *101*, 7827–7832.

Zhang, Y., Wang, P., Shao, W., Zhu, J.-K., and Dong, J. (2015). The BASL polarity protein controls a MAPK signaling feedback loop in asymmetric cell division. Dev. Cell *33*, 136–149.

Zoulias, N., Harrison, E.L., Casson, S.A., and Gray, J.E. (2018). Molecular control of stomatal development. Biochem. J. *475*, 441–454.

Table 10. **Raw root length measurements for bHLH061 ox and bHLH093 ox.** Absolute values of root lengths from individual plants for each genotype. Sample size was not consistent for all genotypes as indicated. All measurements are in mm. bHLH061 ox root length differed in a significant manner from WT (Figure 9).

bHLH061 ox n = 28 Avg = 23.7	bHLH093 ox n = 30 Avg = 17.9	WT n = 10 Avg = 16.6
28	16	19
17	32	10
13	12	22
29	13	16
10	15	20
26	16	19
30	17	11
32	18	22
32	17	11
29	16	16
25	14	
29	17	
31	14	
26	30	
30	26	
29	25	
9	11	
22	12	
17	27	
16	31	
12	27	
13	28	
12	14	
30	15	
29	11	
27	15	
22	12	
37	11	
	16	
	11	

Table 11. **Summary of the significance of flowering traits in bHLH061 ox and bHLH093 ox**. Significance of the average number of leaves at first inflorescence, the average number of days at first inflorescence, and the average number of initial inflorescences in plants overexpressing bHLH061 or bHLH093 compared to WT. Significance is indicated by an asterisk based on a Student's t-test with $p \leq 0.05$. Ectopic overexpression of either bHLH061 or bHLH093 produced a significant change in phenotype across these parameters.

	Average number of leaves at first inflorescence	Average number of days at first inflorescence	Average number of inflorescences per plant
bHLH061 ox	*	*	*
bHLH093 ox	*	*	*

```
bHLH093    ------------------------------------------------------------    0
bHLH061    ------------------------------------------------------------    0
bHLH033    -----MNSDGVWLDGSGESPEVNNGEAASWVRNP-----------DEDWFNNPPPPQ---    41
bHLH116    MGLDGNNGGGVWLNGGGGEREE--NEEGSWGRNQEDGSSQFKPMLEGDWFSSNQPHPQDL    58


bHLH093    ------------------------------------------------------------    0
bHLH061    ------------------------------------------------------------    0
bHLH033    --HTNQNDFRFNGGFPLNPSENLLLLLQQSIDSSSSSSSPLLHPFTLDAASQQQQQQQQQQ    99
bHLH116    QMLQNQPDFRYFGGFPFNPNDNLLL--QHSIDSSSSCSPS-QAFSLDPSQ----------    105


bHLH093    --MELSTQMNVFEELLVPTKQETTDNNINNLSFNGGFDHHHH---QFFPNGYNIDYLCFN    55
bHLH061    ----------METELTQLRKQ--ESN--NLNGVNGGFM-AID---QFVPNDWNFDYLCFN    42
bHLH033    EQSFLATKACIVSLLNVPTINNNT-F--DDFGFDSGFLGQQFHGNHQSPNSMNFTGLN--    154
bHLH116    QNQFLSTNNNKGCLLNVPSSANPF-DNAFEFGSESGFLNQIH-----APISMGFGSLT--    157
                          *          . :.**           *  .:  *


bHLH093    NEEEDENTLLY--PSSFMDLISQPPPLLLHQPP--------PLQPLSPPLSSSATAGATF    105
bHLH061    NLLQEDDNIDHPSSSSLMNLISQPPPLLHQPPQ--------PSSPL----YDSPPLSSAF    90
bHLH033    ---------------HSVPDFLPAPE----------------------NSSGSCGLSPLF    177
bHLH116    ---QLGNRD----LSSVPDFLSARSLLAPESNNNNTMLCGGFTAPLELEGFGSPANGGFV    210
                          *. :::                           .*    .  .


bHLH093    DY--PFLEALQEIIDSSSSSPPLILQNGQEEN-------------FNN------------    138
bHLH061    DY--PFLED---IIHSSYSPPPLILPASQENT-------------NN-------------    119
bHLH033    SNRAKVLKPL-QVMASSGSQPTLFQKRAAMRQSSSSKMCNSESSSEMRKSSYEREIDDTS    236
bHLH116    GNRAKVLKPL-EVLASSGAQPTLFQKRAAMRQSSGSKMGNSESSGM-RRFSDDGDMD---    265
             .      .*:      :: ** : * *:    . .


bHLH093    -------PMSYPSPLMESDQSKSFSVGYCGGETNKKKSKKLEGQPSKNLMAERRRRKRLN    191
bHLH061    ----------YSPLMEESK--SF--ISIGETNKKRSNKKLEGQPSKNLMAERRRRKRLN    164
bHLH033    TGIIDISGLNYESDDHNT-----------N----NNKGKKKGMPAKNLMAERRRRKKLN    280
bHLH116    ETGIEVSGLNYESDEINESG-KAAESVQIGG----GGKGKKKGMPAKNLMAERRRRKKLN    320
                    *   :                  . * :* *;**********;**


bHLH093    DRLSMLRSIVPKISKMDRTSILGDAIDYMKELLDKINKLQDEEQELGNSNNSHHSKLFGD    251
bHLH061    DRLSLLRSIVPKITKMDRTSILGDAIDYMKELLDKINKLQEDEQELGSNSH---------    215
bHLH033    DRLYMLRSVVPKISKMDRASILGDAIDYLKELLQRINDLHTELESTPP-----SSSSLHP    335
bHLH116    DRLYMLRSVVPKISKMDRASILGDAIDYLKELLQRINDLHNELESTPPGSLPPTSSSFHP    380
           *** :***.****:****:*********:****::**.*:  : :.


bHLH093    LKDL------NANEPL---------VRNSPKFEIDRR-DEDTRVDICCSPKPGLLLSTVN    295
bHLH061    LSTL------ITNESM---------VRNSLKFEVDQR-EVNTHIDICCPTKPGLVVSTVS    259
bHLH033    LTPTPQTLSYRVKEELCPSSSLPSPKGQQPRVEVRLREGKAVNIHMFCGRRPGLLLSTMR    395
bHLH116    LTPTPQTLSCRVKEELCPS-SLPSPKGQQARVEVRLREGRAVNIHMFCGRRPGLLLATMK    439
           *.         .:*  :        :. :.*:  *    ..:.: *  :***:::*:


bHLH093    TLETLGLEIEQCVISCFSDFSLQASCSEGAEQRDFITSEDIKQALFRNAGYGGSCL    351
bHLH061    TLETLGLEIEQCVISCFSDFSLQASCFEVGEQRYMVTSEATKQALIRNAGYGGRCL    315
bHLH033    ALDNLGLDVQQAVISCFNGFALDVFRAEQCQEDHDVLPEQIKAVLLDTAGYAGLV-    450
bHLH116    ALDNLGLDVQQAVISCFNGFALDVFRAEQCQEGQEILPDQIKAVLFDTAGYAGMI-    494
           :*:.***:::*.*****..*:*:.    *  ::   :  :  * .*: .***.*
```

Figure 4. **Full sequence alignment of the proteins of subgroup IIIb of Arabdidopsis bHLH proteins**. The sequence alignment was generated by Clustal Omega. Amino acid identity is indicated by asterisks under the alignment. The amino acids N-E-R (green highlight) are the amino acids most critical for DNA binding (Heim et al., 2003) and are present in all four bHLH IIIb subgroup members. The leucines (blue highlight) are believed to be necessary for dimerization and are present in all four of the proteins of subgroup IIIb. Solid red line above the alignment indicates the basic region, red dashed line indicates the helix-loop-helix region. Sequences were obtained from TAIR (https://www.arabidopsis.org).

Figure 5. **Gene Diagrams for At5g10570 (*bHLH061*) and At5g65640 (*bHLH093*)**. (a) Diagram of the At5g10570 gene. The ORF is 1526 base pairs in length and consists of four exons and three introns. Start (ATG) and Stop (TAG) codons are indicated. (**b**) Diagram of the At5g65640 gene. The gene is 1768 base pairs in length and consists of four exons and three introns. Start (ATG) and stop (TAA) codons are indicated. The gene product is the protein bHLH093. Solid black boxes indicate exons, thin black lines indicate introns. Publicly annotated 5' and 3' Untranslated regions (UTR) are indicated to scale.

a

1   2   3   4   5   6   7   8   9   10   11

bHLH061 primers   *bHLH093* primers

b

1   2   3   4   5   6   7   8

c
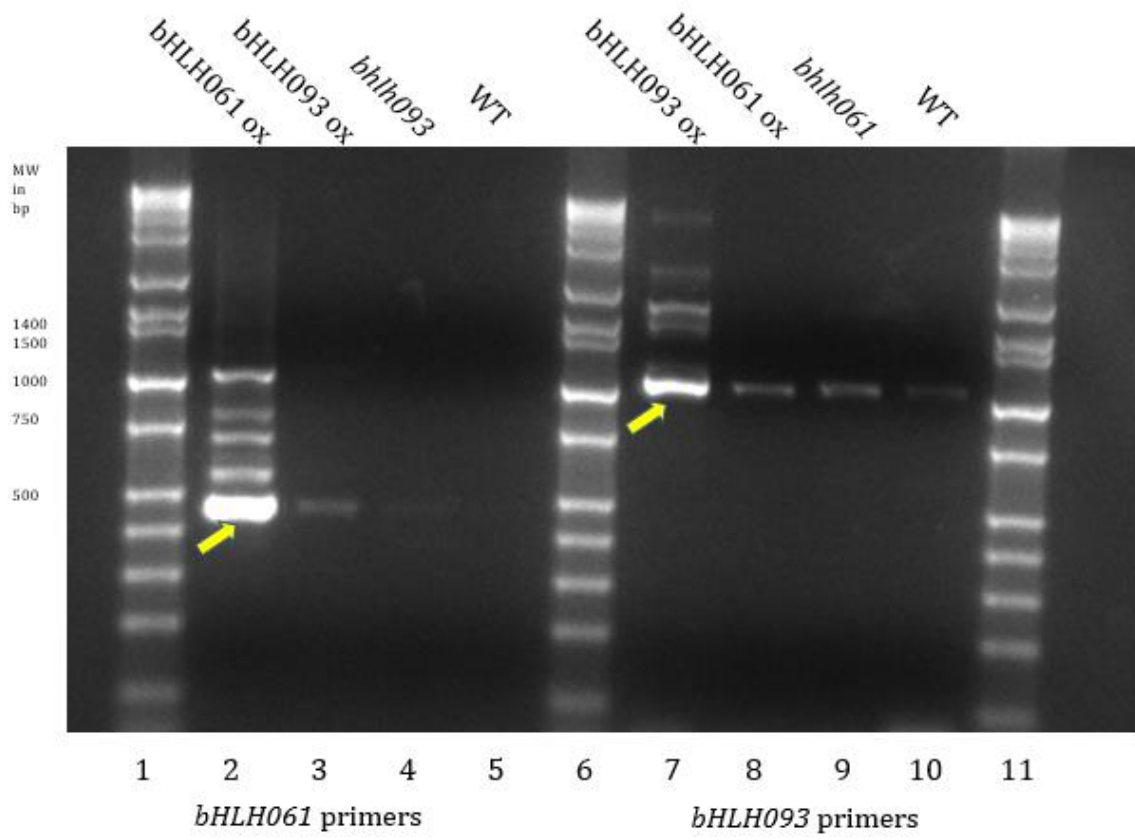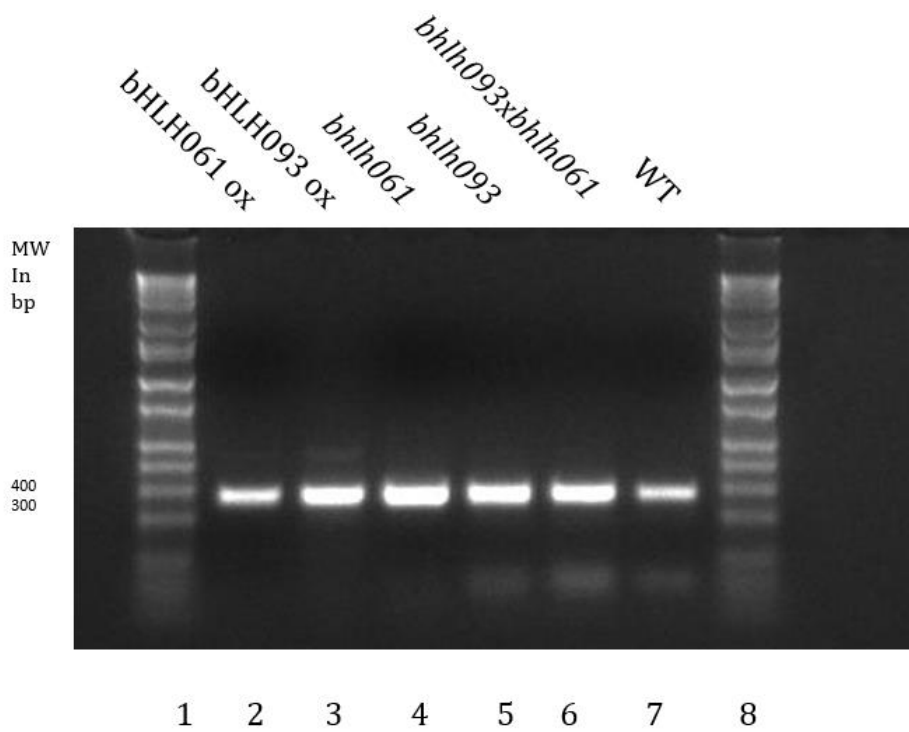
	Forward primer	Reverse Primer	Expected size, bp
bHLH061 transcript	bHLH61_504	bHLH61_1523.rc	460
bHLH093 transcript	bHLH93_1.GW	bHLH93_1765.rc	1053
Actin transcript	ACT 2-1	ACT 2-2	349

Figure 6. **Determination of *bHLH061* and *bHLH093* transcript abundance via RT-PCR**. (**a**) RT-PCR was performed to amplify bHLH093 and bHLH061 transcripts across several genotypes as indicated. Overexpression of the *bHLH061* and *bHLH093* transcripts (lane 2 and 7 vs lane 5 and 10, respectively) was confirmed in the T4 generation via endpoint RT-PCR. Arrow indicates appropriate size for amplicon. Additional higher molecular bands are present in bHLH061 ox and bHLH093 ox, which were not investigated to verify sequence. Lanes 3 and 8 show the presence of bHLH061 transcripts in bHLH093 ox and bHLH093 transcripts in bHLH061 ox as expected. *bhlh093* and *bhlh061* were used as negative controls. Actin was used as a positive control and shown in panel b. b) RT-PCR was performed to amplify actin transcripts as a positive control across several genotypes as indicated. (**c**) Summary of the primers used and the expected sizes in bp of each amplicon.

Final height at senescence
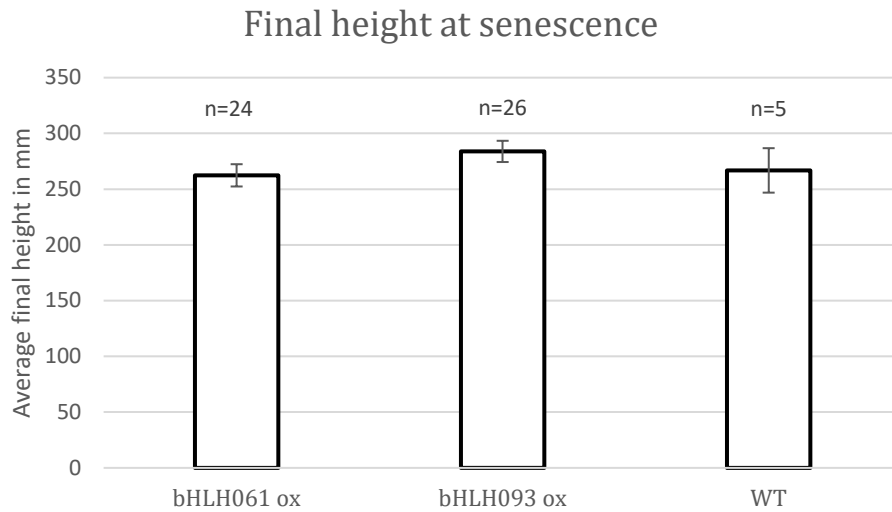
Figure 7. **Final plant height at start of senescence for bHLH061 ox and bHLH093 ox**. Average plant height was measured at seed set. Values are the average height for each genotype. Final plant height did not differ from WT for either bHLH061 ox or bHLH093 ox. n indicates the number of plants evaluated for each genotype. Significance was assessed with Bonferroni correction, $p \leq 0.025$. bHLH061ox p=0.853, bHLH093 ox p=0.473, evaluated using Student's t-test. Vertical lines represent the mean +/- SE.

Figure 8. **Root measurement conditions**. Representative image of WT seedling germinated on MS media for approximately 10days. Media plate was positioned at near vertical position throughout germination. In this position, roots grow on the surface of the media (red bracket) and can be directly measured with minimal manipulation. Scale bar = 1cm.
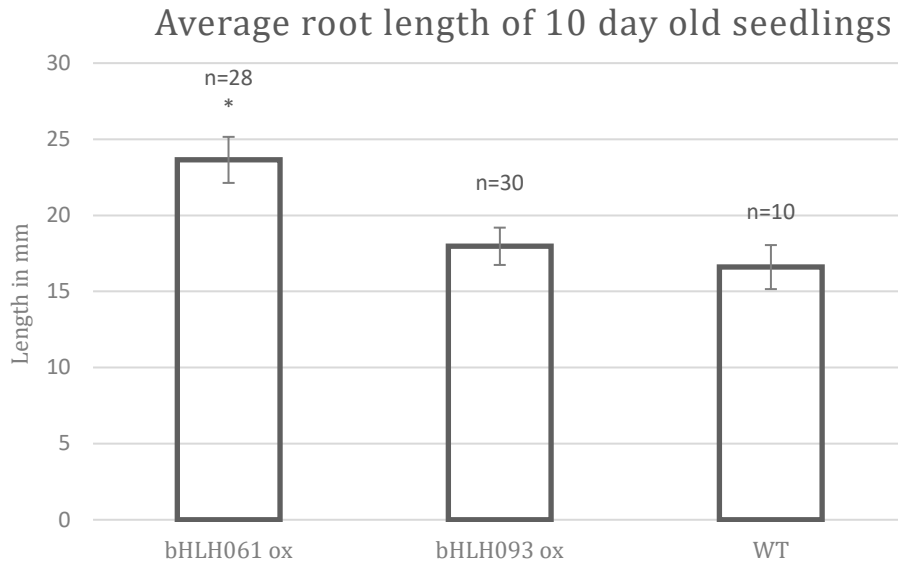
Figure 9. **Average root length of bHLH061 ox and bHLH093 ox seedlings**. Root length measurements of individual seedlings across all genotypes were made at 10 days after plating. n indicates the number of plants evaluated for each genotype. The root length of bHLH061 ox is significantly larger than WT. n indicates the number of plants evaluated for each genotype. Asterisk (*) indicates significance with Bonferroni correction, $p \leq 0.025$. bHLH061 ox $p = 0.013$, bHLH093 ox $p = 0.554$, evaluated using Student's t-test. Vertical lines represent the mean +/- SE.

Average number of leaves at first inflorescence
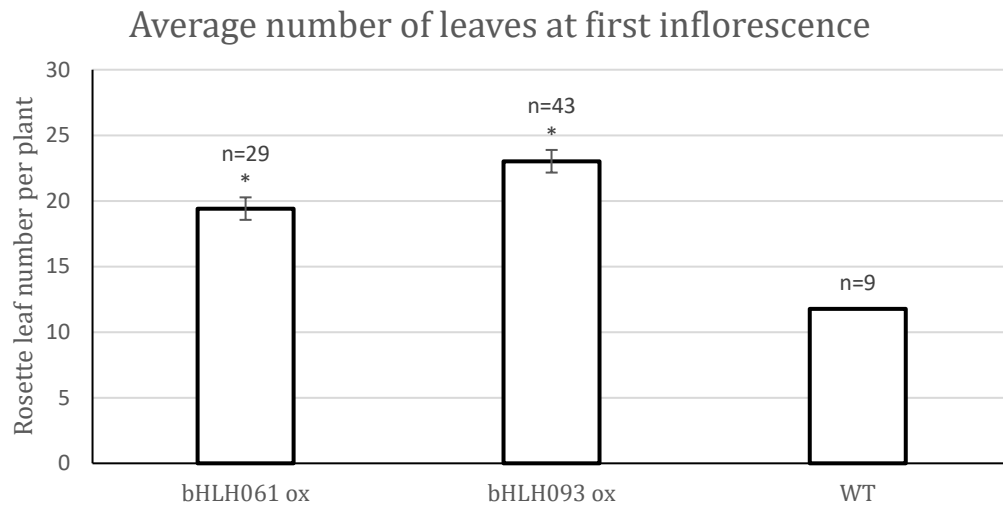
Figure 10. **Average number of leaves at first inflorescence for bHLH061 ox and bHLH093 ox**. The number of true leaves on each rosette was counted at the time of first flower emergence. bHLH061 ox and bHLH091 ox produce more leaves at first inflorescence compared to WT. n indicates the number of plants evaluated for each genotype. Asterisk (*) indicates significance with Bonferroni correction, $p \leq 0.025$. bHLH061ox $p=2.99 \times 10^{-5}$, bHLH093 ox $p=3.90 \times 10^{-7}$, evaluated using Student's t-test). Vertical lines indicate the mean +/- SE.
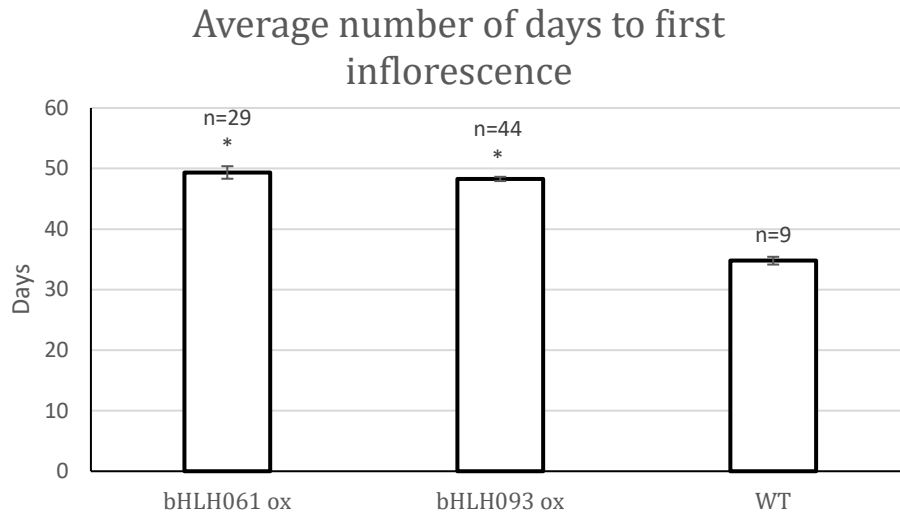
Figure 11. **Average number of days to flowering for bHLH061 ox and bHLH093 ox.** The time in days was measured across all genotypes for the appearance of a first inflorescence. bHLH093 ox and bHLH061 ox flowered later than WT. n indicates the number of plants evaluated for each genotype. Asterisk (*) indicates significance with Bonferroni correction, $p \leq 0.025$. bHLH061 ox $p=4.91 \times 10^{-9}$, bHLH093 ox $p=1.52 \times 10^{-21}$, evaluated using Student's t-test. Vertical lines indicate the mean +/- SE.

Figure 12. **Flowering phenotype of bHLH061 ox and bHLH093 ox**. Images were taken approximately 50 days post plating for bHLH061 ox and bHLH093 ox, and 35 days for WT. Emerging inflorescences are indicated with white arrowheads. bHLH061 ox and bHLH093 ox consistently produce multiple inflorescences. Scale bar = 1cm.
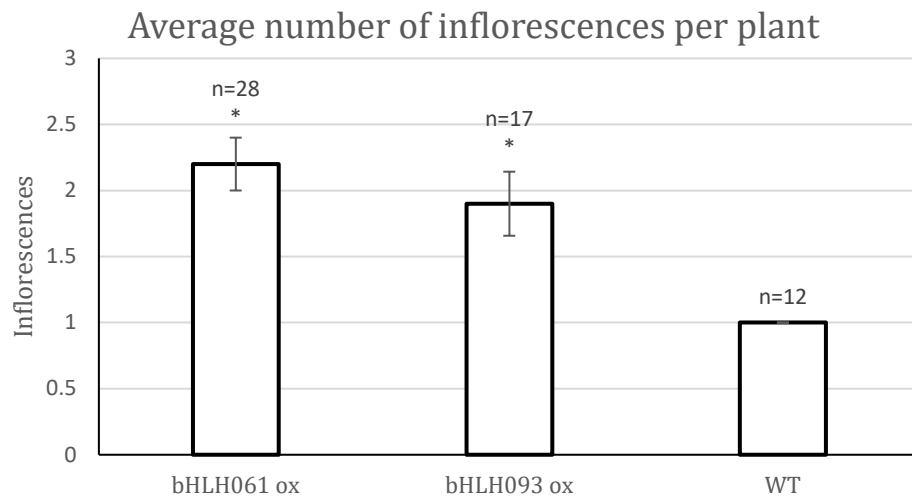
Figure 13. **Average number of inflorescences for bHLH061 ox and bHLH093 ox**. The number of inflorescences was determined when they first emerged across all genotypes as indicated. bHLH061 ox and bHLH093 ox produce more initial inflorescences compared to WT (Figure 12). n indicates the number of plants evaluated for each genotype. Asterisk (*) indicates significance with Bonferroni correction, $p \leq 0.025$. bHLH061 ox $p=1.96 \times 10^{-6}$, bHLH093 ox $p=8.47 \times 10^{-10}$, evaluated using Student's t-test. Vertical bars indicate mean +/- SE.

Figure 14. **Light microscopy images of the abaxial leaf epidermis of bHLH061 ox, bHLH093 ox and WT.** Images were taken of true leaves of approximately 20-day-old seedlings. Across all genotypes, stomata did not display visible structural anomalies compared to WT. Scale bar = 50 μm.
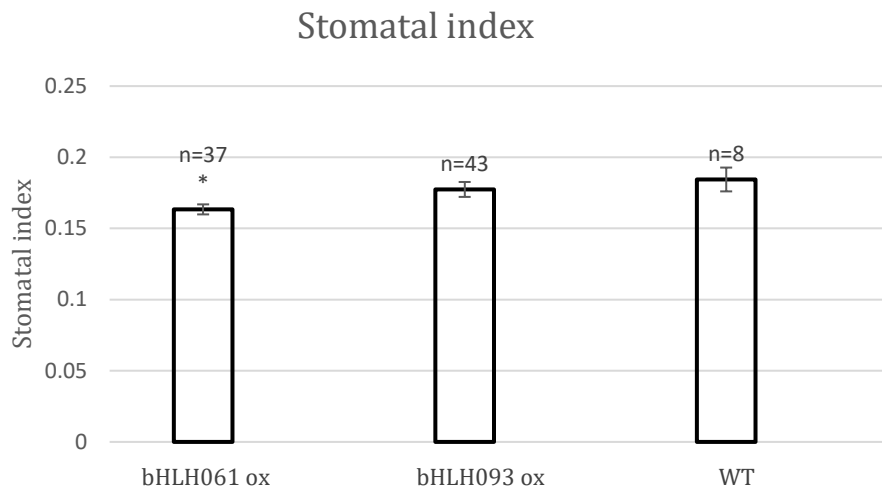
Figure 15. **Average stomatal index (SI) for the bHLH061 ox and bHLH093 ox**. SI is used over absolute number of stomata to normalize against variation in total cell division. bHLH061 ox has a decrease in SI compared to WT. n indicates the number of leaves evaluated for each genotype. Asterisk (*) indicates significance with Bonferroni correction, $p \leq 0.025$. bHLH061 ox $p=0.017$, bHLH093 ox $p=0.585$, evaluated using Student's t-test. Vertical bars indicate mean +/- SE.

.
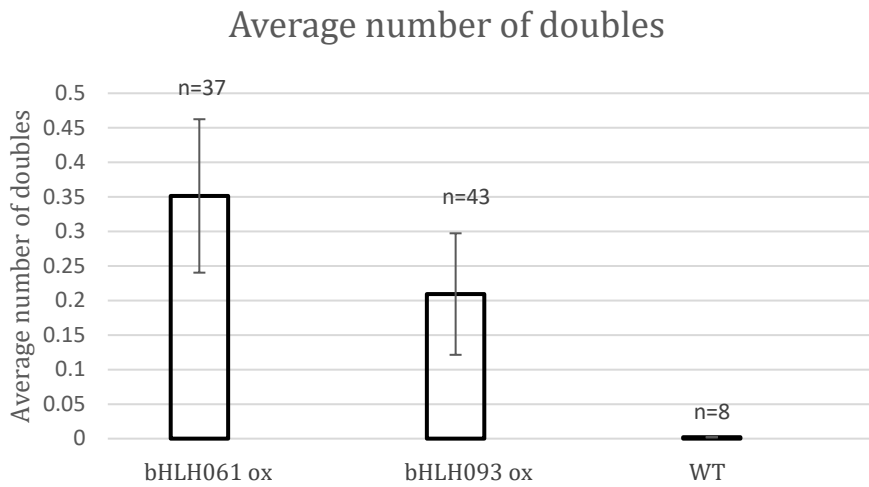
Figure 16. **Average number of stomatal doubles for the bHLH061 ox and bHLH093 ox**. Any two adjacent stomata observed on the abaxial leaf surface was counted as a stomata double. Very few were identified in any of the genotypes. No difference in the absolute number of stomata doubles was observed across genotypes. n indicates the number of leaves evaluated for each genotype. Significance was assessed with Bonferroni correction, $p \leq 0.025$. bHLH061 p=0.152, bHLH061 p=0.280, evaluated using Student's t-test. Vertical bars indicate mean +/- SE.
.
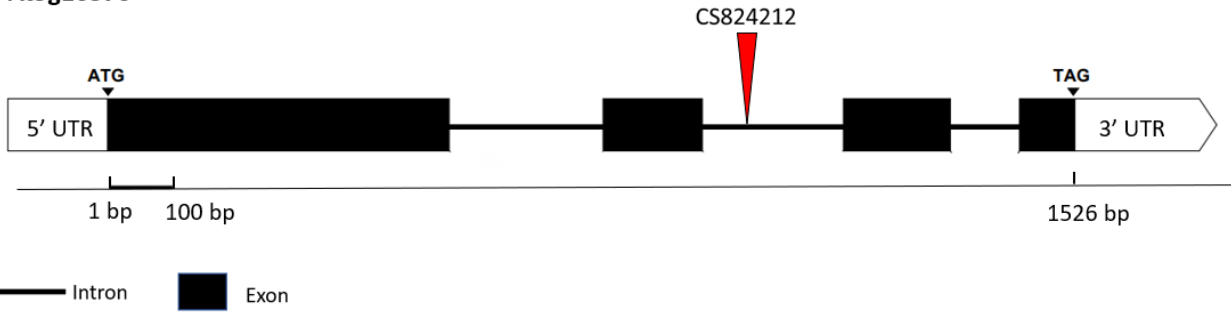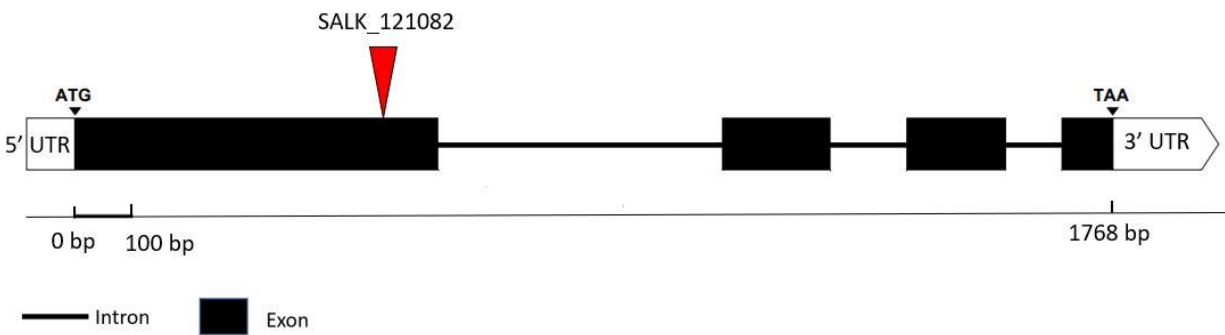
Figure 17. **Gene structure of At5g10570 and At5g65640 and location of T-DNA insertion.** (a) Diagram of the At5g10570 gene and relative location of the CS824212 T-DNA insertion site. (**b**) Diagram of the At5g65640 gene and relative location of the T-DNA insertion (SALK_121082) site. UTR = Untranslated region. Start and stop codons are indicated. T-DNA insertion sites are indicated by red triangle.

Verification of CS824212
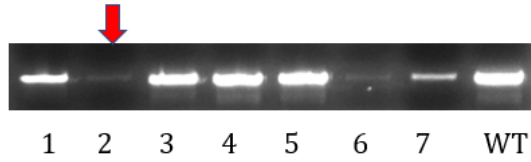
Gene specific primers for At5g10570
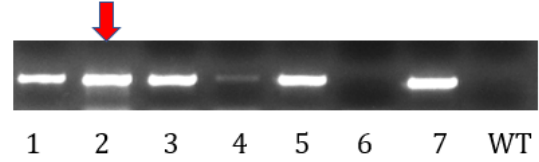
Gene specific forward and T-DNA border primers

b

Verification of SALK_121082
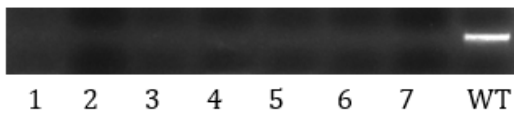
Gene specific primers for At5g65640
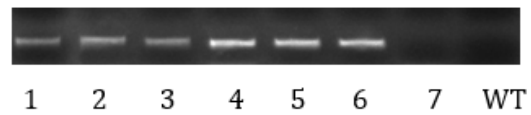
Gene specific forward and T-DNA border primers

c

	Gene-Specific Primers	Expected size (bp)	Gene-specific and Left Border (LB) primers	Expected size (bp)
CS824212/*bhlh061*	bHLH61_1.GW-bHLH61_1526.rc	1526	bHLH61_1.GW-SAILLB3	1100
SALK_121082/*bhlh093*	bHLH93_1.GW -bHLH93_1768.rc	1768	bHLH93_1.GW-LBA1	511

Figure 18. **PCR verification of T-DNA inserts.** PCR was used to verify the relative location of the T-DNA insertion for SALK_121082 and CS824212. Both *bhlh061* and *bhlh093* lines produced clear PCR amplification products consistent with the annotated insertion location (Figure 17). (**a**) Verification of the CS824212 insertion site in At5g10570. DNA was extracted from 7 different plants segregating for the T-DNA insertion (Lanes 1-7). Gene-specific primers amplify a 1526 bp fragment of the *bHLH061* gene if it is uninterrupted. Gene and LB primers amplify a fragment of the T-DNA sequence if it is present. Plant 2

(Lane 2) shows no product amplification using the gene-specific primers (left panel, red arrow) indicating the lack of the uninterrupted At5g10570 gene. Gene/LB primers produce an amplification product (right panel, red arrow) indicating the presence of the T-DNA insertion. Plant 2 was confirmed to be a homozygous carrier of the At5g10570 T-DNA insertion. Progeny from plant 2 (*bhlh061*) were used for further analysis.
(**b**) Verification of the SALK_121082 insertion site in At5g65640. DNA was extracted from 7 different plants segregating for the T-DNA insertion (Lanes 1-7). Gene-specific primers amplify a 1768 bp fragment of the *bHLH093* gene if it is uninterrupted. Gene and LB primers amplify a fragment of the T-DNA sequence if it is present. Plants 1-7 (lanes 1-7) show no product amplification using the gene-specific primers (left panel) indicating the lack of the uninterrupted At5g10570 gene. Plants 1-6 (lanes 1-6) show amplification products using gene/LB primers indicating the presence of the T-DNA insertion. Plants 1-6 were confirmed to be homozygous carrier for the SALK_121082 T-DNA insertion (right panel). Progeny from homozygous plants (*bhlh093*) were used for further analysis. WT DNA was used as the positive control for gene-specific primer reactions, and as a negative control for the T-DNA border reactions. (**c**) Table of primer pair names used for insert verification and expected product sizes (bp).

a

bHLH061 gene specific primers

bHLH093 gene specific primers

MW

3000

1000

500

1 2 3 4

bHLH061 ox

bhlh061

bhlh093xbhlh061

1 2 3 4

bHLH093 ox

bhlh093

bhlh093xbhlh061

b

MW In bp

400
300

1 2 3 4 5 6 7 8

bHLH061 ox

bHLH093 ox

bhlh061

bhlh093

bhlh093xbhlh061

WT

c
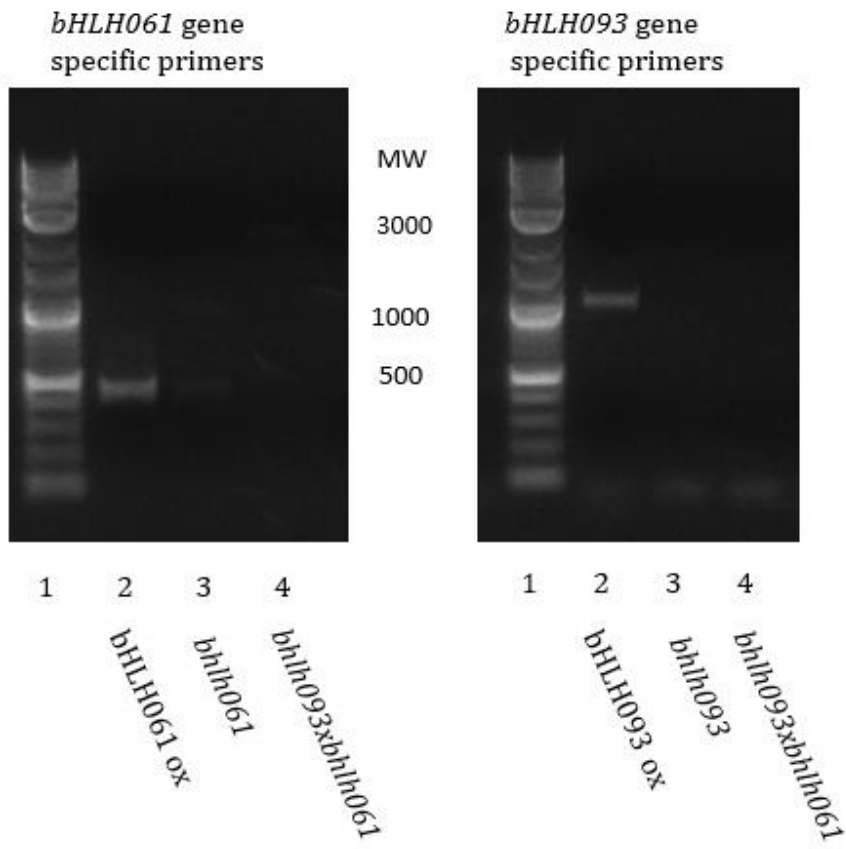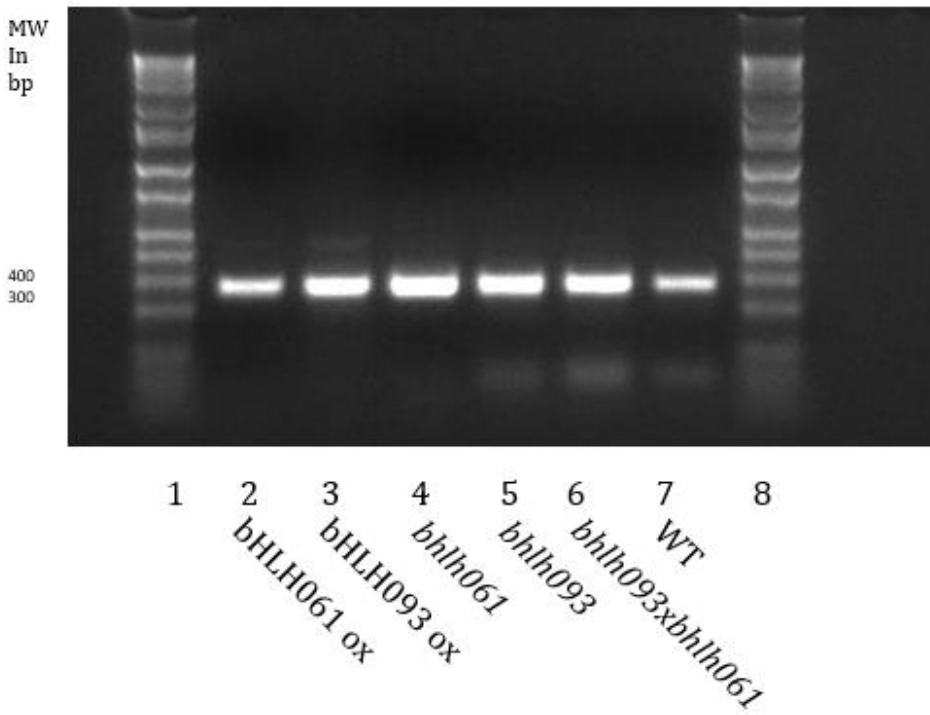
	Forward primer	Reverse Primer	Expected size if present, bp
bHLH061	bHLH61_504	bHLH61_1523.rc	460
bHLH093	bHLH93_1.GW	bHLH93_1765.rc	1053
Actin (control)	ACT 2-1	ACT 2-2	349

d

	bHLH061 gene-specific primers		bHLH093 gene-specific primers		Actin-specific primers	
	Expected	Observed	Expected	Observed	Expected	Observed
bHLH061 ox (control)	Y	Y			Y	Y
bhlh061	N	N			Y	Y
bHLH093 ox (control)			Y	Y	Y	Y
bhlh093			N	N	Y	Y
bhlh093xbhlh061	N	N	N	N	Y	Y

Figure 19. **Confirmation of loss of transcripts in *bhlh061*, *bhlh093*, and *bhlh093xbhlh061***. Lack of expression of the *bHLH061* and *bHLH093* transcripts in *bhlh061*, *bhlh093*, and *bhlh093xbhlh061* plants was confirmed in the F3 generation via endpoint RT-PCR. (**a**) Total RNA and first strand cDNA were obtained from *bhlh061*, *bhlh093,* and *bhlh093xbhlh061* plants. RT-PCR was performed to amplify bHLH093, bHLH061, and actin transcripts as indicated. bHLH061 ox and bHLH093 ox (lanes 2 and 6) were used as positive control. There were no *bHLH061* transcripts in *bhlh061* mutant plants (lane 3), no *bHLH093* transcripts in *bhlh093* mutant (lane 7), and neither transcript was present in the *bhlh093xbhlh061* double mutant (lanes 4 and 8). (**b**) ACT2 was used as positive control for RNA integrity (Note: this figure is identical to Figure 6.b). (**c**) Table of the names of primers used and expected amplicon size for each reaction. (**d**) Summary of expected and observed results. Results indicate none of the T-DNA insertion mutants produce detectable transcripts for their respective genes.
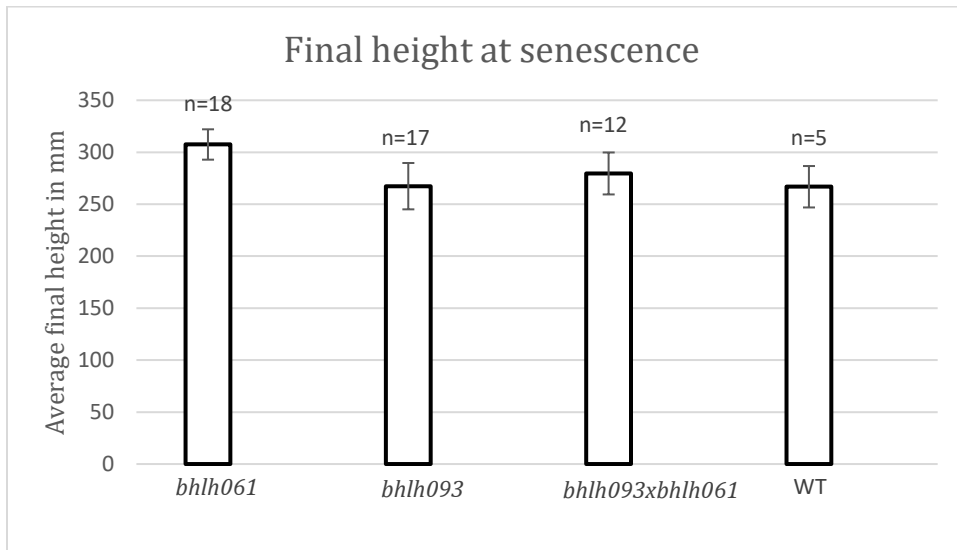
Figure 20. **Final plant at start of senescence *for bhlh061, bhlh093,* and *bhlh093xbhlh061***Average plant height was measured at seed set. Values are the average height for each genotype. Final plant height did not differ from WT for *bhlh061*, *bhlh093*, or *bhlh093xbhlh061*. n indicates the number of plants evaluated for each genotype. Significance was assessed with Bonferroni correction, $p \leq 0.017$. *bhlh061* p = 0.188, *bhlh093* p=0.990, *bhlh093xbhlh061* p=0.714, evaluated using Student's t-test. Vertical lines represent the mean +- SE.
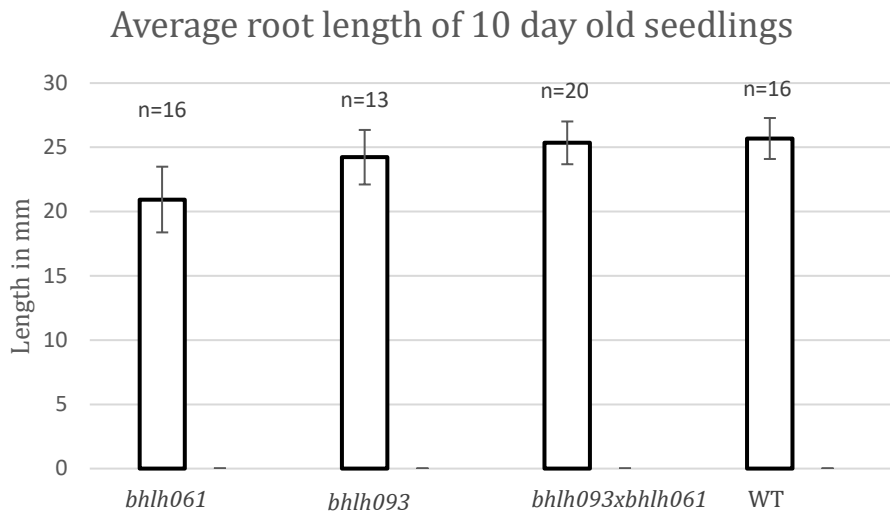
Figure 21. **Average root length for *bhlh061*, *bhlh093*, and *bhlh093xbhlh061***. Root length measurements of individual seedlings across all genotypes were made at 10 days after germination (Figure 8). The average root length of *bHLH061*, *bHLH093*, and *bHLH093xbHLH061* did not differ from WT, though *bhlh016* has a shorter average root length than the other genotypes. n indicates the number of plants evaluated for each genotype. Significance was assessed with Bonferroni correction, p ≤ 0.017. *bhlh061* p = 0.125, *bhlh093* p=0.580, *bhlh093xbhlh061* p=0.886, evaluated using Student's t-test. Vertical lines represent the mean +/- SE.

Average number of leaves at first inflorescence
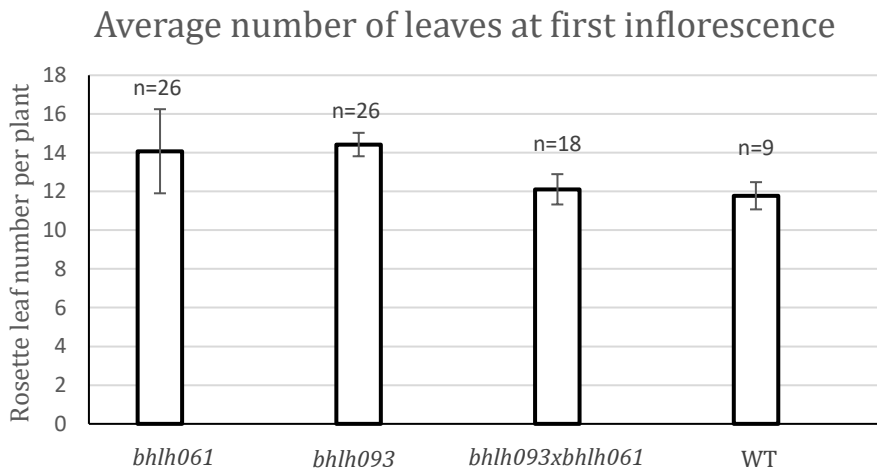
Figure 22. **Average number of leaves at first inflorescence for *bhlh061, bhlh093,* and *bhlh093xbhlh061***. The number of true leaves on each rosette was counted at the time of first flower emergence. While *bhlh061* and *bhlh093* showed an increase in the average number of leaves compared to WT, it was not significant. The double knockout line showed very little difference from WT. n indicates the number of plants evaluated for each genotype. Significance was assessed with Bonferroni correction, $p \leq 0.017$. *bhlh061* p = 0.544, *bhlh093* p=0.024, *bhlh093xbhlh061* p=0.618, evaluated using Student's t-test. Vertical lines indicate the mean +/- SE.
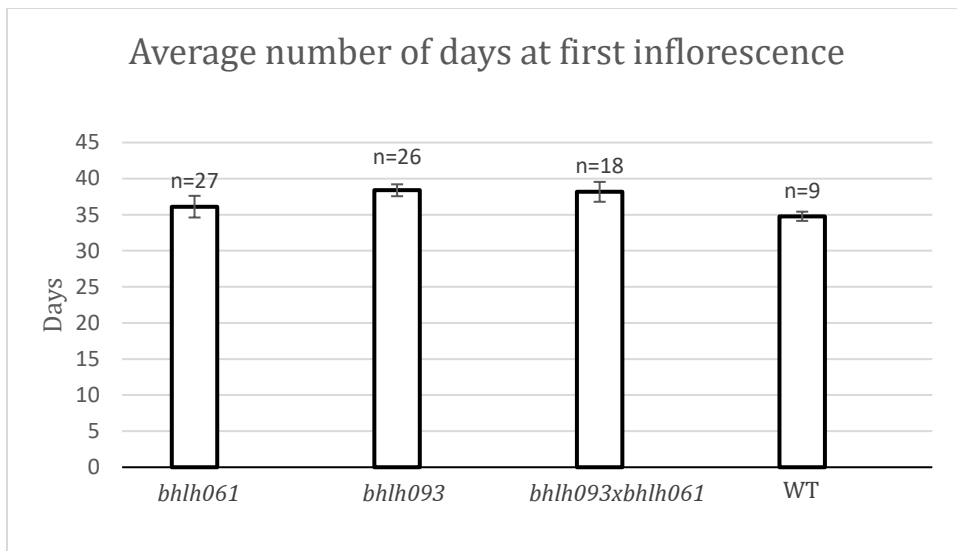
Figure 23. **Average number of days to first inflorescence for *bhlh061, bhlh093,* and *bhlh093xbhlh061***. The time in whole days before observation of a first inflorescence was measured for all genotypes. *bhlh093* flowered later than *bhlh061* and *bhlh093xbhlh061*. While the time difference compared to WT is not statistically significant the average number of days is similar for all genotypes (36, 38, 38, 35 respectively). n indicates the number of plants evaluated for each genotype. Significance was assessed with Bonferroni correction, $p \leq 0.017$. *bhlh061* $p = 0.618$, *bhlh093* $p=0.019$, *bhlh093xbhlh061* $p=0.105$, evaluated using Student's t-test. Vertical lines indicate the mean +/- SE.

Average number of inflorescences per plant
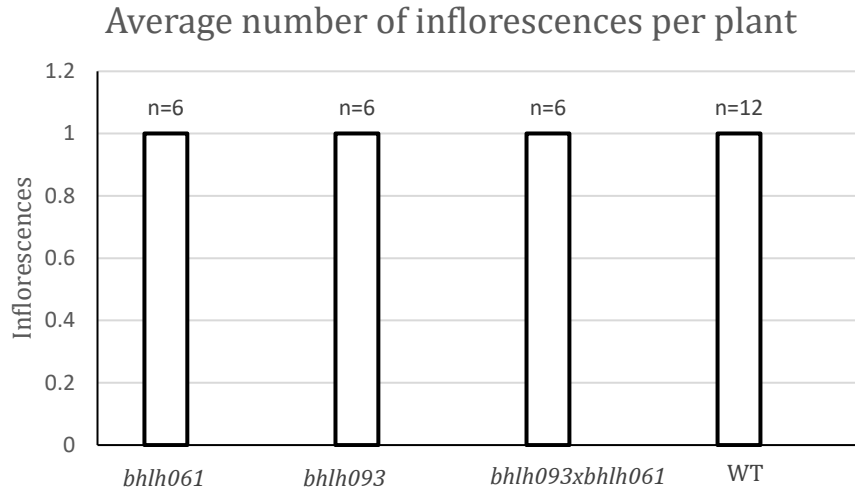
Figure 24. **Average number of inflorescences for *bhlh061, bhlh093,* and *bhlh093xbhlh061.*** The number of flower buds at first inflorescence was evaluated for all genotypes. All genotypes showed one inflorescence, which is the expected result for WT. n indicates the number of plants evaluated for each genotype. Vertical lines indicate the mean +/- SE.
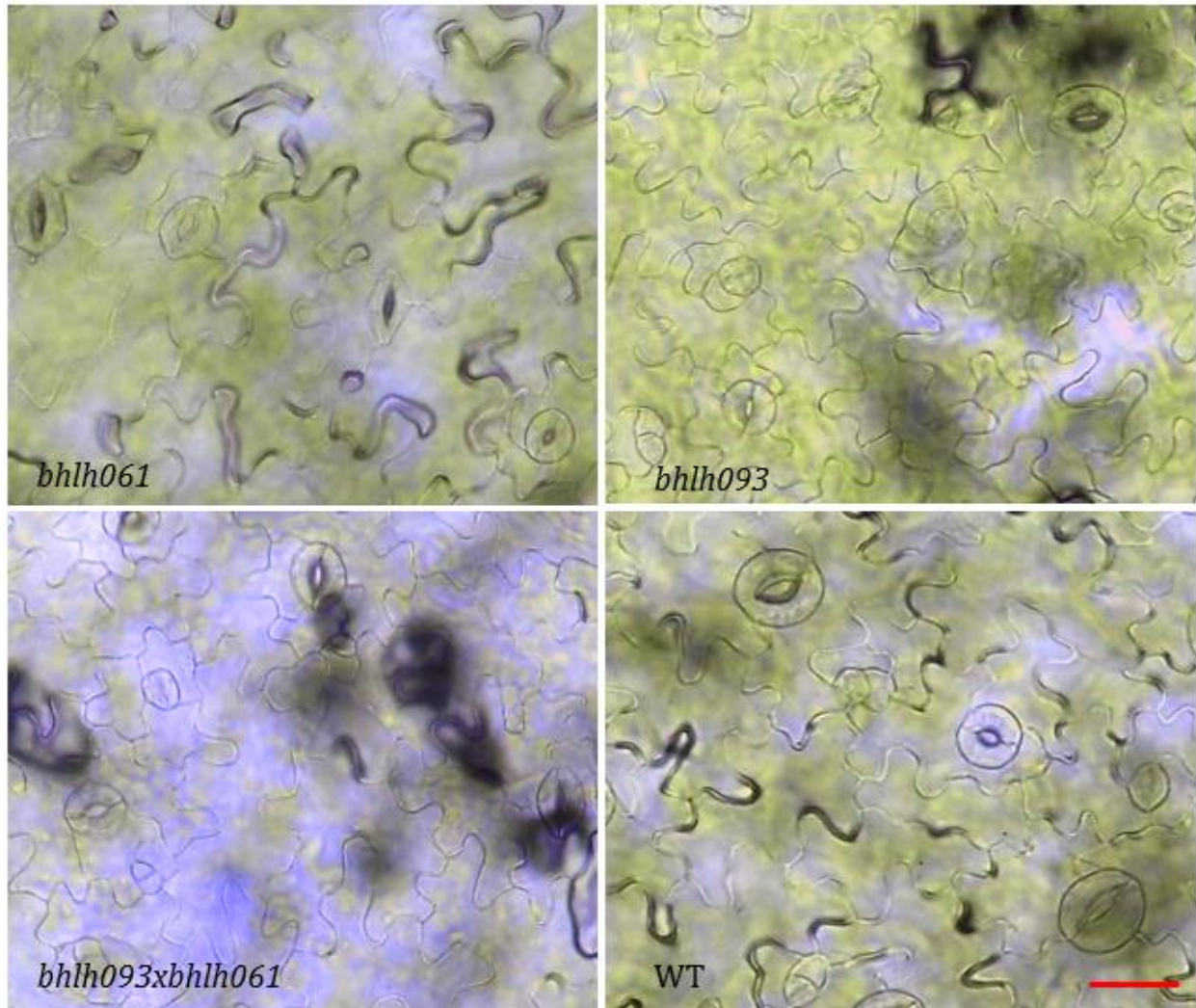
 Figure 25. **Light microscopy images of the abaxial leaf epidermis of *bhlh061*, *bhlh093*, *bhlh093xbhlh061*, and WT.** Images were taken of true leaves of approximately 20-day old seedlings. No anomalies in stomatal structure were observed compared to WT. Scale bar = 50 μm.
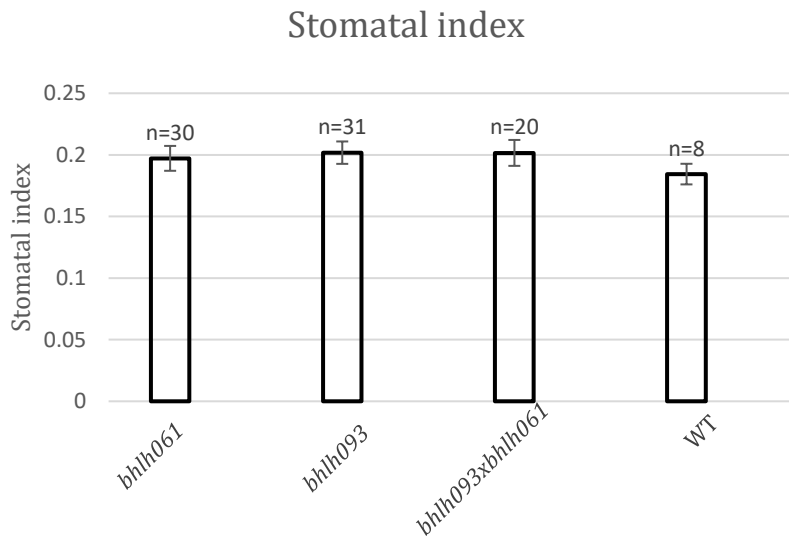
Figure 26. **Average stomatal index for *bhlh061*, *bhlh093*, and *bhlh093xbhlh061*.** SI is used over absolute number of stomata to normalize against variation in total cell division. SI for *bhlh061, bhlh093*, and *bhlh093xbhlh061* does not differ in a significant manner from WT. n indicates the number of leaves evaluated for each genotype. Significance was assessed with Bonferroni correction, p ≤ 0.017. *bhlh061* p = 0.531, *bhlh093* p=0.354, *bhlh093xbhlh061* p=0.337, evaluated using Student's t-test. Vertical lines indicate the mean +/- SE.
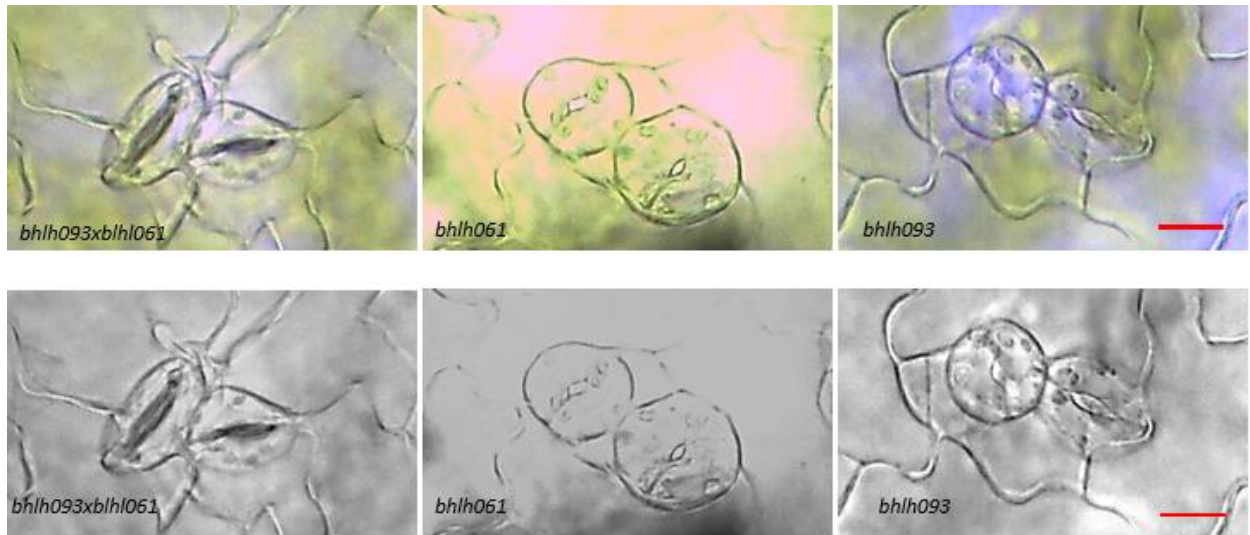
Figure 27. **Light microscopy images of stomatal doubles on the abaxial leaf epidermis of *bhlh061, bhlh093* and *bhlh093xbhlh061***. A significant number of stomatal doubles were observed in *bhlh061, bhlh093*, and *bhlh093xbhlh061*. There were none observed for WT. Scale bar = 50 μm.
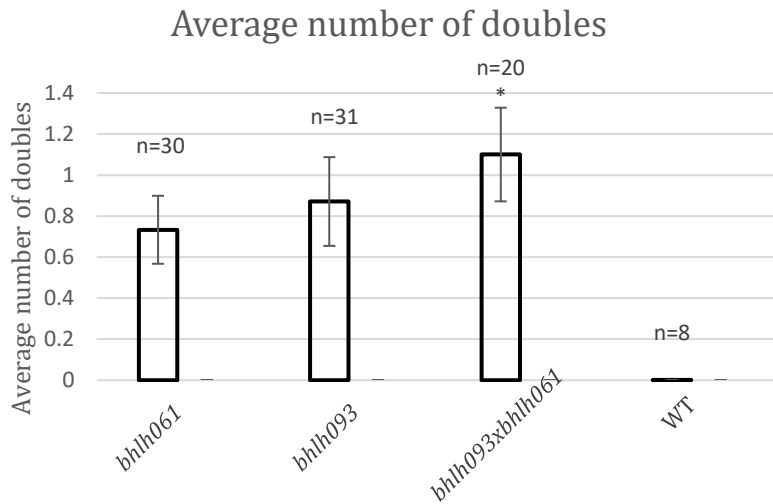
Figure 28. **Average number of doubles for *bhlh061*, *bhlh093*, and *bhlh093xbhlh061***.
The average number of doubles was calculated for each *bhlh061*, *bhlh093*, and
bhlh093xbhlh061. The average number of doubles for *bhlh093xbhlh061* is larger than WT.
n indicates the number of leaves evaluated for each genotype. Asterisk (*) indicates
significance with Bonferroni correction, $p \leq 0.017$. *bhlh061* p = 0.030, *bhlh093* p=0.05,
bhlh093xbhlh061 p=0.005, evaluated using Student's t-test). Vertical lines indicate the
mean +/- SE.